ORIGIN OF THE SOLAR SYSTEM

I: *Gravitational Contraction of the Turbulent Protosun and the Shedding of a Concentric System of Gaseous Laplacian Rings*

A. J. R. PRENTICE

Dept. of Mathematics, Monash University, Clayton, Victoria, Australia

(Received 16 May, 1978)

Abstract. A theory for the origin of the solar system, which is based on ideas of supersonic turbulent convection and indicates the possibility that the original Laplacian hypothesis may by valid, is presented.

We suggest that the first stage of the Sun's formation consisted of the condensation of CNO ices (i.e. H_2O, NH_3, CH_4, . . .) and later H_2, including He as impurity atoms, at interstellar densities to form a cloud of solid grains. These grains then migrate under gravity to their common centre of mass giving up almost two orders of magnitude of angular momentum through resistive interaction with residual gases which are tied, via the ions, to the interstellar magnetic field. Grains rich in CNO rapidly dominate the centre of the cloud at this stage, both giving up almost all of their angular momentum and forming a central chemical inhomogeneity which may account for the present low solar neutrino flux (Prentice, 1976). The rest of the grain cloud, when sufficiently compressed to sweep up the residual gases and go into free fall, is not threatened by rotational disruption until its mean size has shrunk to about the orbit of Neptune.

When the central opacity rises sufficiently to halt the free collapse at central density near $10^{-13}\,\mathrm{g\,cm^{-3}}$, corresponding to a mean cloud radius of $10^4 R_\odot$, we find that there is insufficient gravitational energy, for the vaporized cloud to acquire a complete hydrostatic equilibrium, even if a supersonic turbulent stress arising from the motions of convective elements becomes important, as Schatzman (1967) has proposed. Instead we suggest that the inner 3–4% of the cloud mass collapses freely all the way to stellar size to release sufficient energy to stabilize the rest of the infalling cloud. Our model of the early solar nebula thus consists of a small dense quasi-stellar core surrounded by a vast tenuous but opaque turbulent convective envelope.

Following an earlier paper (Prentice, 1973) we show how the supersonic turbulent stress $\langle \rho_t v_t^2 \rangle = \beta \rho GM(r)/r$, where β is called the turbulence parameter, ρ is the gas density and $M(r)$ the mass interior to radius r causes the envelope to become very centrally condensed (i.e. drastically lowers its moment-of-inertia coefficient f) and leads to a very steep density inversion at its photosurface, as well as causing the interior to rotate like a solid body. As the nebula contracts conserving its angular momentum the ratio Θ of centrifugal force to gravitational force at the equator steadily increases. In order to maintain pressure equilibrium at its photosurface, material is extruded outwards from the deep interior of the envelope to form a dense belt of non-turbulent gases at the equator which are free of turbulent viscosity. If the turbulence is sufficiently strong, we find that when $\Theta \to 1$ at equatorial radius $R_e = R_0$, corresponding to the orbit of Neptune, the addition of any further mass to the equator causes the envelope to discontinuously withdraw to a new radius $R_e < R_0$, leaving behind the circular belt of gas at the Kepler orbit R_0. The protosun continues to contract inwards, again rotationally stabilizing itself by extruding fresh material to the equator, and eventually abandoning a second gaseous ring at radius R_1, and so on. If the collapse occurs homologously the sequence of orbital radii R_n of the system of gaseous Laplacian rings satisfy the geometric progression

$$R_n/R_{n+1} = [1 + m/Mf]^2 = \text{constant}, \qquad n = 0, 1, 2, \ldots,$$

analogous to the Titius-Bode Law of planetary distances, where m denotes the mass of the disposed ring and M the remaining mass of the envelope. Choosing a ratio of surface to central temperature for the envelope equal to about 10^{-3} and adjusting the turbulence parameter $\beta \sim 0.1$ so that R_n/R_{n+1}

The Moon and the Planets 19 (1978) 341–398.

matches the observed mean ratio of 1.73, we typically find $f = 0.01$ and that the rings of gas each have about the same mass, namely $1000M_{\oplus}$ of the solar material. Detailed calculations which take into account non-homologous behaviour resulting from the changing mass fraction of dissociated H_2 in the nebula during the collapse do not appreciably disturb this result. This model of the contracting protosun enables us to account for the observed physical structure and mass distribution of the planetary system, as well as the chemistry. In a later Paper II we shall examine in detail the condensation of the planets from the system of gaseous rings.

1. Introduction

1.1. THE LAPLACIAN HYPOTHESIS AND ITS DIFFICULTIES

According to the hypothesis originally proposed by Laplace in 1796, the planets are supposed to have condensed from a concentric system of circularly orbiting gaseous rings which the young proto-Sun abandoned at its equator whenever the centrifugal force overcame the gravitational force during its primordial contraction from interstellar density. For full details of this hypothesis and other related theories of the solar system we refer the reader to the papers of ter Haar and Cameron (1963) and ter Haar (1967). Here, for the moment, we consider the main difficulties which confront the development of this simple and attractive hypothesis.

(i) *Angular Momentum Difficulty*

One of the main obstacles which face the Laplacian hypothesis is the distribution of angular momentum in the solar system.. It was recognized by Babinet (1861) that the planetary system is far too light in mass compared to the Sun in order for the latter to have contracted to its present size in the manner suggested by Laplace. If, for example, the angular momentum of the entire solar system is stored back into the Sun, the ratio of centrifugal force to gravitational force at the equator, if the Sun be re-expanded to the orbit of Neptune, barely rises to 1% of the required amount. Later Hoyle (1955) and other workers (Urey, 1951; Kuiper, 1951), pointed out that this objection is by no means as severe as Babinet's calculation implied, since the present distribution of planetary material is only a relic of what originally would have been present when the planets were formed, if the planets were created from solar material.

Table I shows the relative abundances of the main types of planetary material present in $1000M_{\oplus}$ ($M_{\oplus}$ = mass of the Earth) of material of solar composition derived from the recent compilation of solar abundance data of Engvold and Hauge (1974).

To account for planets like Uranus and Neptune which are thought to consist largely of ices, and perhaps a rocky centre, and which have masses $15M_{\oplus}$ and $17M_{\oplus}$ respectively, we see we shall require an equivalent mass of about $1000M_{\oplus}$ of solar material at each of these orbits. Similarly considering the rock-like terrestrial planets and bearing mind that the efficiency of accumulation of condensates probably varies from one orbit to the next (Whipple, 1972) we also find that we require roughly comparable masses of solar material at each orbit, again perhaps as much as $1000M_{\oplus}$. Thus the total amount of mass which the protosun shed in forming the planetary system may have been as much as $10^4M_{\oplus}$

TABLE I

Main chemical constituents of 1000 $M_\oplus$ solar material

Type	Constituent	Unit of mass
gaseous	H, He	982
ice-like	C, N, O (as hydrides), Ne, Ar	13
rocky	Mg, Al, Si, Fe (as oxides) Ni, etc	5
Total		1000

(i.e., 3% $M_\odot$) or even 6%$M_\odot$ if another 10 or rings of gas were shed between the orbit of Mercury and radius $R_\odot$. These estimates of the mass m_{neb} of the protoplanetary 'nebula' agree precisely with the independent estimates of Whipple (1972), Kuiper (1951) and most cosmochemists.

Schatzman (1949) has written down the equations which govern the amount of material which a uniformly rotating cloud must shed at its equator in order to safely contract while maintaining a Kepler velocity $\sqrt{GM/R_e}$ at its equator of radius R_e. The residual mass M and angular momentum L after the star has shrunk from equatorial radius R_0 to R_e are given by

$$M = M_0[R_e/R_0]^{f/(2-3f)}, \quad L = L_0[R_e/R_0]^{1/(2-3f)} \tag{1}$$

where $f = I/MR_e^2$ is the moment-of-inertia coefficient and I the moment of inertia. Thus taking $m_{\text{neb}} = 0.06M_\odot, R_0 = 10^4 R_\odot$ we see that for the contracting proto-Sun to produce a planetary system as light as the one observed we require that

$$f = \frac{2m_{\text{neb}}}{M_\odot} \Big/ \ln \frac{R_0}{R_\odot} \simeq 0.01. \tag{2}$$

Such a small value of f (for a uniform sphere $f = 0.4$) implies that the internal mass distribution of the proto-Sun must have been such that most of its mass resided near the centre. That is, it must have been very centrally condensed. This conclusion appears to have been reached by most cosmogonists (e.g., Jeans, 1928; p. 397). Unfortunately, our knowledge of stellar interiors does not admit structures with such a low f, at least for those possessing convective interiors. This has been a main obstacle to the development of a modern Laplacian hypothesis. In addition it is not at all clear whether the contracting proto-Sun can maintain a uniform angular velocity throughout its interior as required by Equation (2) for the efficient transfer of angular momentum from its interior. If, as the work of Hayashi (1961) demonstrated, the interior of the gravitationally contracting proto-Sun is fully convective and, as is often loosely assumed, the convective motions eliminate all large-scale differential motions (Roxburgh, 1966) then we are faced with the bug bear that f is about an order of magnitude larger than the required amount, being 0.135 for a fully rotating polytrope of index $n = 1.5$ (James, 1964).

(ii) *Energy Difficulty*

An even more serious difficulty which faces the development of the Laplacian hypothesis is the so-called energy problem first discussed by Cameron (1962). Cameron observed, following the work of Hayashi (1961), that during the interval $10^4 R_\odot$ to $10^2 R_\odot$, corresponding to the range of the planetary system, there is insufficient gravitational energy in the proto-solar cloud to complete the various internal atomic and molecular transitions (dissociation, ionization, etc.) to the levels required for a consistent hydrostatic or thermodynamic equilibrium. This conclusion persists even if one takes into account supersonic turbulent stress arising from the motions of convective elements (Schatzman, 1967, 1971). The free collapse of the proto-Sun from the interstellar density thus cannot be arrested during this interval and so there will be insufficient time for the cloud to eliminate differential rotations in its interior and hence dispose of its excess angular momentum at its equator in the manner proposed by Laplace. This difficulty appears all the more acute if we recall that the resulting orbital eccentricity ϵ of any material shed from the equator of a fully rotating cloud which is contracting with inward radial velocity v_r is $\epsilon = v_r/\sqrt{GM/R_e}$. The near circularity of the planetary orbits thus implies that $v_r \ll \sqrt{GM/R_e}$ and hence that if what Laplace said occurred, then the proto-Sun must have really existed in a near state of hydrostatic equilibrium for $R_e \leqslant 10^4 R_\odot$. What physical processes, therefore, were responsible for energetically stabilizing the proto-Sun first near the orbit of Neptune?

(iii) *The Discreteness Difficulty and the Titius-Bode Law of Planetary Distances*

A further difficulty which faces the Laplacian hypothesis is to explain why the rotating proto-solar cloud should seek to dispose of its excess primordial angular momentum in a discontinuous manner through the discrete detachment of a system of gaseous rings. Surely one would expect the shedding process to occur more or less continuously, as Equation (1) implies, to form a uniformly distributed disc-like nebula in the equatorial plane. The answer to this problem would then perhaps supply an explanation to the so-called Titius-Bode law of planetary distances which, in modern terms, (see ter Haar and Cameron, 1963; ter Haar, 1967; and Nieto, 1972) states that the sequence of successive orbital radii R_n, counting inwards from Neptune ($n = 0$), satisfy an approximately geometric relationship of the form

$$R_n/R_{n+1} \simeq \text{constant} = 1.73. \tag{3}$$

Similar scaling-law relationships hold for the distances of the regular satellites of the major planets from their parent bodies which suggests that the same cosmogonic processes were responsible for the formation of both planetary and satellite systems.

As we shall show later in this paper, if the proto-Sun does dispose of its angular momentum in discrete amounts each of mass m at the sequence of orbital radii R_n ($n = 0, 1, 2, \ldots$) then it follows from the law of conservation of angular momentum that, provided $f \ll 1$, we have the relations

$$M_n \simeq \text{constant} = M, \text{say} \tag{4}$$

$$R_n/R_{n+1} = \{1 + m/Mf\}^2 \tag{5}$$

where M_n is the residual protosolar mass left over after the disposal of the nth ring. Evidently, therefore, equating Equations (3), (5) we see that the Titius-Bode law implies that the masses of the gaseous rings were all about the same, each about $1000 M_\oplus$ of solar material, setting $f = 0.01$. Quite astoundingly, this prediction of roughly comparable masses, together with a condensation temperature T_n which varies as $T_n \propto R_n^{-1}$, coincides precisely with the empirical evidence obtained from the distribution of planetary material. Thus even at this broad level of analysis we see how a Laplacian hypothesis is capable of successfully accounting for both the basic physical and chemical features of the solar system.

(iv) *Condensation and Accumulation Difficulty*

A final set of difficulties which face the adoption of the Laplacian hypothesis is to explain how the single planetary objects which we see today managed to condense and accumulate from the gaseous rings. Certainly it is reasonable to expect that as the rings 'cooled down' the various condensates appropriate to the temperature at each orbital radius would precipitate to form circularly orbiting streams of rocks and ice, which we may call planetesimals. Indeed the work of ter Haar (1948, 1950), Hoyle and Wickramasinghe (1968), Lewis (1974) and Grossman and Larimer (1974) has convincingly demonstrated how the chemistry of the planetary system can be explained in terms of a variation with distance R_n of the black-body temperature $T_n \propto R_n^{-1}$ due to the Sun at the time of condensation of each planet. In the inner regions of the solar system where $R \leqslant 10^2 R_\odot$ and $T \geqslant 1000\,\text{K}$ we would expect to find terrestrial-like planets consisting mostly of iron, magnesium and aluminium silicates (see Table I). In the outer regions where, say, $r \gtrsim 10^3 R_\odot$ and $T \lesssim 150\,\text{K}$ ices rapidly form so that we would expect planetary compositions similar to those of Uranus and Neptune. Presumably Jupiter and Saturn first formed this way but then were successful in capturing large amounts of H and He (ter Haar, 1948; Hoyle,1960).

Granted then that the chemistry of the solar system is compatible with the Laplacian picture, the problem is to explain how the orbiting streams of planetesimals managed to aggregate together to form single planetary objects at each orbital radius R_n. The work of Maxwell (1855) on the stability of Saturn's rings cast doubts upon the possibility of such an accumulation occurring. We should also bear in mind the theorem of Poincaré (1911) that the rings of gas themselves have the tendency to scatter into space under the disruptive influence of their own rotation, if they rotate with uniform angular velocity. The formation of the different types of satellites should also be considered alongside the aggregation problem.

1.2. Outline of Papers and Ideas

In this paper and the following one we present an account of the physical processes which we feel were responsible for the origin of the solar system and which, we believe, gives

grounds for accepting the validity of the original Laplacian hypothesis. Because the Sun's formation was probably typical of that which occurred for other stars of solar mass in our neighbourhood of the Galaxy, in the next section of this paper we discuss the general difficulties of star formation, especially the obstacles which confront the commonly-held notion that stars are formed form the gravitational collapse of interstellar clouds of gas and dust. Instead of the gas cloud hypothesis we follow Reddish and Wickramasinghe (1969; see also Prentice and ter Haar, 1971) and investigate what would happen, if the first stage of the Sun's formation took place in a portion of a very dark region of a large interstellar cloud of total mass $\simeq 10^4 M_\odot$ and density $10^{-20}\,\mathrm{g\,cm^{-3}}$ (i.e., $n_\mathrm{H} \simeq 10^4\,\mathrm{atom\ cm^{-3}}$) where the temperature may have fallen sufficiently low ($\lesssim 5\,\mathrm{K}$) for the condensation of H_2 and the other gases, including He, onto existing particles of dust to form a cloud of solid grains, each of mean radius about $10^{-4}\,\mathrm{cm}$.

We examine in detail the migration of these grains towards their common centre of mass taking into account the dynamical friction between the grains and the residual uncondensed atoms and molecules of the cloud, which are mostly neutrally ionized. Prentice and ter Haar (1971) have shown that these neutral atoms are prevented from co-collapsing with the grain cloud because of the frictional coupling between them and the ionic component of the gas which is rigidly anchored to the galactic magnetic field. In this way the grain cloud is capable of giving up almost two orders of magnitude of angular momentum so that the resulting protostellar object does not become rotationally unstable until its radius has shrunk to about the orbit of Neptune. Long before this radius is reached, however, the grain cloud sweeps up the residual gases of the cloud and goes into free fall. We also consider the differential segregration of grain material with respect to chemical composition as a result of the variation of the drag coefficient $\gamma \propto 1/\rho_s a$ with intrinsic grain density ρ_s for grains of constant radius a or mass. Prentice (1976) has suggested that an enhancement of the relative concentration of grains rich in C, N and O towards the centre of the cloud at this stage may have important bearings both on the solar neutrino problem and the geological evolution of the Earth.

In Section 3 we study the physical changes which take place in the gravitationally collapsing proto-solar cloud when the central density rises to about $10^{-13}\,\mathrm{g\,cm^{-3}}$, corresponding to a surface radius $\simeq 10^4 R_\odot$ for a uniform cloud of solar mass, and the cloud becomes opaque and begins to heat up through compression. Dissociation of H_2 and subsequent ionization of H and He prevent a halt in the free collapse of the cloud at this stage, however (Cameron, 1962). Following a suggestion of Schatzman (1967) we consider the possibility that the cloud may be energetically stabilized through the development of a large supersonic turbulent stress, using the theory of supersonic turbulent convection developed by Prentice (1973). As this mechanism proves insufficient we then consider the possibility, following Larson (1969), that the free collapse may be halted if a small fraction of its central mass collapses all the way through to normal stellar size to form a dense compact core thus liberating an additional supply of gravitational energy. Calculations are performed using simple polytropic structures but taking into account the variation of the polytropic index with changing mass fraction of dissociated H in the cloud.

Our model of the initial proto-solar cloud thus consists of a small central luminous metal-rich core of mass $\simeq 0.03 M_\odot$ and density $\simeq 10^{-3}\,\mathrm{g\,cm^{-3}}$ surrounded by a tenuous but opaque supersonically-turbulent energetically-stabilized rotating convective envelope of radius $\simeq 10^4 R_\odot$ and mass $\simeq 1 M_\odot$ and normal composition. In Section 4 we consider in detail the influence of the supersonic turbulent stress, arising from the motions of buoyant convective elements, on the physical structure of the rotating proto-solar envelope. Following an earlier paper (Prentice, 1973) we show how the stress drastically lowers the moment-of-inertia coefficient f as required by the Laplacian hypothesis, and leads to the formation of a dense outer shell of non-turbulent gas beyond the photo-surface where the heat developed by the cloud during its gravitational contraction can ultimately be freely radiated away under conditions of nearly uniform temperature.

We also demonstrate how the supersonic convective motions create a large turbulent viscosity which eliminates all differential rotation inside the envelope. Below the photo-surface the material therefore rotates like a rigid body but beyond this surface, where the turbulent viscosity is zero, the gas conserves its angular momentum rather than angular velocity. We compute the positions of the outer equipotential surfaces of the cloud and show that as the rotation parameter $\Theta_e = \omega_e{}^2 R_e^3/GM$ increases towards unity, where ω_e, R_e are the equatorial angular velocity and radius, the outer shell of non-turbulent gas assumes an essentially ring-like structure at the equator with most of its mass residing outside the equatorial photocylinder $s = R_e$, where s is the cylindrical polar radius.

In Section 5 we study the rotational evolution of the proto-solar envelope as it contracts towards the radius R_0 where the centrifugal force at the equator first balances the gravitational force (i.e., $\Theta_e = 1$) and the outermost shell of non-turbulent gas evolves into a ring-like structure at the equator. In Section 6 we consider in detail the processes which occur near the equator as the proto-Sun continues to contract inwards from the radius R_0, its internal distribution of pressure with density being maintained by the convection. We find that for a sufficiently large degree of turbulent stress, measured by the turbulence parameter β (Prentice, 1973), the amount of non-turbulent gas which can be stored at the equator is so large that when the star contracts beyond the radius R_0, the extrusion of further material to the equator under conditions of uniform rotation causes the outer convective layers of the critically rotating envolope to discontinuously withdraw to a new equatorial radius $R_e < R_0$ where $\Theta_e < 1$, thus rotationally stabilizing the envelope. The polar radius remains unchanged. The non-turbulent gases beyond the photocylinder are unable to co-rotate with the convective interior as they have no viscous coupling. We thus show that this material is discontinuously abandoned by the contracting envelope and that it subsequently distributes itself evenly about the circular Keplerian orbit $s = R_0$ to form a complete torus, or Lapacian ring, of orbiting gas, in which the pressure gradient is balanced by the centrifugal force and the gravitational field of the Sun.

We show how the proto-solar envelope, rotationally stabilized by the shedding of a discrete gaseous ring at radius R_0, continues to contract inwards eventually becoming

rotationally unstable again at a new radius R_1, satisfying Equation (5), where a second gaseous ring is in turn shed. The whole process repeats itself again and again until the collapse is halted when the cloud acquires normal stellar size.

In Section 7 we compute the variation of the various physical characteristics (m, f, etc.) of the fully rotating envelope as a function of the degree of turbulence and central-to-photosurface temperature ratio at various stages of the contraction, paying special attention to non-homologous effects arising from the changing mass fraction of dissociated H in the cloud, but ignoring the influence of the small central embryonic core. We compute the rate of contraction of the envelope paying special attention to the final stages of the Kelvin-Helmholtz contraction, when photosurface conditions cause the surface temperature of the cloud to level off to about 4500 K, thus drastically reducing the rate of collapse, and causing the supersonic turbulence to die down.

In Paper II we shall study the condensation of the planets from the rings of gas. There we compute the chemical species expected at each orbit and consider the physical processes which lead to the accumulation and aggregation of the planetesimals into single protoplanetary objects. We examine the subsequent gravitational contraction of these objects to form compact planetary cores. We also consider the influence of the young Sun's radiation on the physical evolution and dispersal of the uncondensed gases, mostly H and He, of each Laplacian ring, and investigate the possible capture and gravitational contraction of the residual gases onto the planetary cores of mass $m_c \sim 10 M_\oplus$ of the outer planets to form regular satellite systems in precisely similar manner to the contraction of the proto-solar envelope. The spins of the terrestrial planets, the formation of the asteroids, comets, irregular satellite and ring systems, and other anomalies of the solar system will also be considered.

2. Early Stages of the Sun's Formation and the Grain Cloud Hypothesis

2.1. THE DIFFICULTIES OF STAR FORMATION

It is generally believed that stars are formed through the gravitational collapse of interstellar clouds of gas and dust. It is also known (Mestel, 1965a, 1965b; Spitzer, 1968; Prentice and ter Haar, 1971) that it is very difficult to reconcile this hypothesis with the observed distribution of angular momentum and magnetic and thermal energy of the interstellar material. Consider, for example, the physical state of a portion of solar mass of a large interstellar cloud of mass $\geqslant 10^3 M_\odot$ and of average hydrogen atom number density $n_{\mathrm{H}} = 20\,\mathrm{cm}^{-3}$. Assuming a helium/hydrogen atom number ratio $n_{\mathrm{He}}/n_{\mathrm{H}} = 0.1$ and a metal abundance $Z = 0.02$ gives the cloud a mean mass density $\rho_i = 4.8 \times 10^{-23}\,\mathrm{g\,cm}^{-3}$. The radius R_i of a roughly spherical portion of solar mass is 0.7 pc. Because the angular velocity of the Galaxy in the neighbourhood of the Sun is $8 \times 10^{-16}\,\mathrm{s}^{-1}$ and the local galactic shear -0.6 (Schmidt, 1965), yielding a net local angular velocity $\omega_i = 3 \times 10^{-16}\,\mathrm{s}^{-1}$, the angular momentum of the typical portion is

$$L_i = \tfrac{2}{5} M_\odot R_i^2 \omega_i = 1.1 \times 10^{54}\,\mathrm{g\,cm^2\,s^{-1}}. \tag{6}$$

Next consider the angular momentum of a star of solar mass and size which is rotating so rapidly that the centrifugal force at the equator equals the gravitational force, so that

$$\Theta \equiv \omega^2 R_e^3 / GM = 1, \tag{7}$$

where Θ is called the rotation parameter, and ω denotes the angular velocity which is assumed to be uniform and R_e is the equatorial radius. If the star is centrally condensed it assumes a lenticular shape when $\Theta = 1$ with $R_e = \frac{3}{2} R_p$, where the polar radius R_p is hardly influenced by rotation (Jeans, 1928; Monaghan and Roxburgh, 1965). Setting $R_p = R_\odot$, the maximum angular momentum of the star is thus seen to be

$$L_{\max} = M_\odot f \sqrt{G M_\odot R_e} = 1.0 \times 10^{50}\,\mathrm{g\,cm^2\,s^{-1}}, \tag{8}$$

where for a fully rotating Sun the moment-of-inertia coefficient is $f = f_\odot (R_p/R_e)^2 \simeq 0.03$ since $f_\odot = 0.062$ (Allen, 1962). Thus we see than in order for a typical interstellar cloudlet of solar mass to collapse to normal stellar size it will be necessary for it to dispose of four orders of magnitude and angular momentum.

Consider now the magnetic and thermal energy difficulties. For a typical interstellar cloud in the neighbourhood of the Sun, the magnetic field is $B_i = 3 \times 10^{-6}$ G and the temperature about $T = 100$ K (Spitzer, 1968; p. 170). The magnetic and thermal energy of a cloud of solar mass and radius $R_i = 0.7$ pc are

$$U_{\mathrm{mag}} = \frac{1}{6\mu_0} B_i^2 R_i^3 = 1.5 \times 10^{43}\,\mathrm{erg}, \tag{9}$$

$$U_{\mathrm{kin}} = \frac{3}{2} \frac{\mathscr{R} T}{\mu} M_\odot = 2.5 \times 10^{43}\,\mathrm{erg}, \tag{10}$$

whilst the rotational energy $\frac{1}{2} L_i \omega_i = 2 \times 10^{38}$ erg is insignificant.

In contrast, the self-gravitational energy of the cloud is

$$\Omega_{\mathrm{grav}} = \frac{3}{5} \frac{G M_\odot^2}{R_i} = 7 \times 10^{40}\,\mathrm{erg}. \tag{11}$$

In order that the cloud undergo gravitational collapse to form a star it is necessary that Ω_{grav} exceed the sum of U_{mag} and U_{kin}. Clearly such an event is impossible unless the mass of the cloud exceed about $10^3 M_\odot$. Thus the popular notion that stars are formed from the collapse of portions of interstellar gas clouds is one which must represent a gross oversimplification of the actual physical processes whereby a star is born.

2.2. THE GRAIN-CLOUD HYPOTHESIS

To overcome the energetic difficulties outlined above, Reddish and Wickramasinghe (1968) proposed that stars are formed through the gravitational collapse of solid H_2 grain clouds. In a sufficiently dense region of a very large interstellar gas cloud of mass

$M \geqslant 10^3 M_\odot$ which has undergone free gravitational collapse to a density where, say, $n_H = 10^4\,\mathrm{cm}^{-3}$ and the radius and angular velocity of a fragment of solar mass are

$$R_0 = 0.1\mathrm{pc}, \qquad \omega_0 = \omega_i(R_i/R_0)^2 = 1.5 \times 10^{-14}\mathrm{s}^{-1}, \tag{12}$$

the optical depth to the centre of the cloud may be sufficiently great to prevent the penetration of heat from nearby stars. Rapid cooling of the central region of the cloud may then occur through re-radiation in the infrared of the thermal energy of atoms and molecules impinging on the surfaces of the dust particles. If the temperature can be lowered to 3 K the hydrogen gas can condense out completely onto the dust particles to form grains of solid H_2. Copious condensation of solid mantles of H_2, including helium as impurity atoms, may also occur for $T \leqslant 5$ K but probably not for temperatures larger than 10 K (Hollenbach and Salpeter, 1971). Between 10 K and 20 K, the gases of CO, CO_2, NCO, N_2 and other 'ice-like' substances condense out readily (Duley, 1974) whilst H_2O condenses out at about 100 K. In any event, the resulting cloud of solid grains has neither the thermal or magnetic energy of its former gaseous counterpart and so may freely undergo self-gravitational collapse.

2.3. AN EXTENDED HYPOTHESIS

Prentice and ter Haar (1971) have pointed out that the angular momentum difficulty associated with star formation can also be partly resolved within the grain cloud hypothesis if one takes into account the dynamical friction between the solid grains and the residual uncondensed gases of the cloud. If cosmic rays can penetrate to the centre of the cloud to maintain the equilibrium ionization level in the gas and hence prevent detachment of the magnetic field from the rest of the cloud of mass $10^3 M_\odot$, the ionized component of the fragment of $1 M_\odot$ remains rigidly coupled to the big cloud. As long as the frictional coupling between the neutral and ionic components of the gas exceeds that between the grains and the neutral component, the grains slip through the gas towards their common centre of mass, like beads down the spokes of a wheel, maintaining a uniform angular velocity ω_0. For a uniform cloud having ion number density n_{ion} and initial grain number density $n_{gr}(0)$ this spoke-like collapse continues until the fractional radius $S(t) = r(t)/r(0)$ of the grain cloud has shrunk to the value

$$S_1 = [n_{gr}(0)\pi\bar{a}^2/n_{ion}\sigma_{ion}]^{1/3}, \tag{13}$$

where σ_{ion} stands for the collision cross-section between neutral atoms and ions, due mostly to helium collisions, and $\bar{a}$ the mean grain radius. As soon as $S(t)$ falls below S_1 the grain cloud becomes so compressed that it begins to sweep up the residual neutral gases and goes into free fall. Inserting typical values ($\bar{a} = 1.5 \times 10^{-4}$ cm, $n_{gr}(0)/n_H = 10^{-12}$, etc.) we find that $S_1 \simeq 0.14$. Since the angular momentum of a grain scales as $l \propto S^2(t)$ it follows that almost two orders of magnitude of angular momentum can be lost in this manner. The angular momentum of our fragment of solar mass at the end of the grain braking era is thus about

$$L_f = S_1{}^2 L_i \simeq 10^{52}\,\mathrm{g\,cm^2\,s^{-1}}. \tag{14}$$

The radius of the grain cloud at this stage is about 0.01 pc and the angular velocity $2 \times 10^{-14}\,\mathrm{s^{-1}}$.

The equation of motion of the grain cloud during the period of braking may be written as

$$\ddot{S}(t) = -\frac{k^2}{S^2}\left[\psi + (1-\psi)S^3\right] + \langle\gamma\rangle(1-\psi)\dot{S}(t), \tag{15}$$

where ψ denotes the initial mass fraction of grains in the cloud of total initial density ρ_0 and

$$k^2 = 4\pi G\rho_0/3, \quad \langle\gamma\rangle = \frac{3\rho_0}{\langle\rho_s a\rangle}\left(\frac{\mathscr{R}T}{2\pi\mu}\right)^{1/2}, \tag{16}$$

where $\langle\gamma\rangle$ is the mean coefficient of dynamical friction, $\langle\rho_s a\rangle$ the mean value of $\rho_s a$, ρ_s the density of a grain and T, μ the temperature and mean molecular weight of the uncondensing gases. During conditions of terminal braking ($\ddot{S} \to 0$, $\langle\gamma\rangle/k \simeq 300 \gg 1$) Equation (15) has the solution

$$S(t) = \left[\exp\left(-3k^2 t/\langle\gamma\rangle\right) - \psi\right]^{1/3}/(1-\psi)^{1/3}, \tag{17}$$

from which it follows that the 'collapse time' of the cloud is given by

$$t_c = \frac{\gamma}{3k^2}\ln\left[\psi + S_1{}^3(1-\psi)\right]^{-1} = 2 \times 10\,\mathrm{yr}, \tag{18}$$

if we insert again typical values $\psi = 0.5$, $T = 5\,\mathrm{K}$, $\mu = 2.353$, $\rho_s = 0.11\,\mathrm{g\,cm^{-3}}$, $\rho_0 = 2.3 \times 10^{-20}\,\mathrm{g\,cm^{-3}}$. As soon as the cloud reaches the fractional radius S_1 the collapse proceeds much more rapidly on a free-fall time scale $S_1^{3/2}/k \sim 2 \times 10^4\,\mathrm{yr} \ll t_c$, so that t_c essentially defines the total collapse time.

2.4. NON-UNIFORM ASPECTS OF THE GRAIN-CLOUD COLLAPSE

In the simplified analysis of the dynamical properties of the collapsing grain cloud given above it was assumed that the grains were all identical, both in size and composition. This meant that grains at a given distance $r(t)$ from the centre of the cloud fall at the same rate and that the collapse of the cloud proceeded homologously, so that the relative spacing between all grains is also preserved. If, however, there exist chemical inhomogeneities in the distribution of grain material so that some grains are formed denser than others, or sooner than others as in the case of grains containing large amounts of C, N, O, then segregation of the grain material will occur. This leads not only to enhancement of the relative abundance of the dense metal-rich species C, N, O towards the centre of the cloud but also permits the faster moving grains to give up practically all of their angular momentum by the time the rest of the cloud goes into free fall at radius S_1. We consider both of these non-uniform aspects in detail below.

(i) *Segregation of Grain Material According to Chemical Composition*

Let us consider in detail the parameters which define the descent of a single grain of density ρ_s and radius a which falls from rest at time t_0 and distance $r(t_0)$ from the centre of a uniform gas cloud of density ρ_0. The solution for its distance at time t follows from Equation (17) setting $\psi = 0$ and replacing $\langle\gamma\rangle$ by γ: namely,

$$r(t)/r(t_0) = e^{-k^2(t-t_0)/\gamma} = \exp\left[-\frac{k^2}{\langle\gamma\rangle}(t-t_0)\frac{\rho_s a}{\langle\rho_s a\rangle}\right]. \tag{19}$$

It follows from Equation (19) that grains which have a large value of $\rho_s a$ and hence a low friction coefficient $\gamma \propto 1/\rho_s a$ sink to the centre of the gaseous cloud sooner than the ones with a small $\rho_s a$ value. This is because the former grains experience a smaller drag per unit mass passing through the gas. For grains of constant radius this, of course, means that it is the dense ones which sink the faster. Indeed, since the density of solid H_2 is only $0.089\,\mathrm{g\,cm^{-3}}$ compared to the value of 1 to $2\,\mathrm{g\,cm^{-3}}$ for 'ice-like' or metal-rich grains consisting primarily of CO, CO_2, N_2, N_2O, H_2O, etc (Duley, 1974), these latter grains will sink to the centre of the cloud much more quickly than solid H_2 grains of the same radius. The same result is true when one considers grains of a given mass since in this case $\rho_s a \propto \rho_s^{2/3}$ which again favours the denser grains.

We therefore propose that even if the cloud of grains is initially everywhere chemically homogeneous on the average, segregation of grain material will occur according to the distribution of chemical composition amongst individual grains. Thus as the grains fall, the concentration of metals will progressively increase towards the centre of the cloud, and decrease at the outside, leading to a final composition profile which is spatially inhomogeneous. In addition since the 'ice-like' grains containing the metals C, N and O condense out sooner than the H_2 grains, further enrichment of these materials towards the centre of the cloud is expected because these grains commence their journey sooner.

We should of course stress that the above argument does not prove that the centre of the final collapsed object will consist only of heavy elements or, conversely, that the surface consists purely of hydrogen. Firstly, it is probably only a small proportion of the grains which consist purely of one species or the other whilst the majority of grains contain mixtures of both. Secondly, we have assumed that the grains each have either the same radius or mass. A pure H_2 grain can reduce its friction coefficient $\gamma \propto 1/\rho_s a$ and travel as fast as a very dense grain if its radius is say 10 to 20 times larger than the mean value $\bar{a}$, though this seems exceptional. Hence, strictly speaking, the segregation process which we have discussed occurs according to the distribution of γ rather than grain density, though as we have suggested the one usually implies the other. Thirdly, we have yet to consider the later stages of proto-stellar evolution when convective mixing may replenish the envelope of the protostar with material from the outer mantle of the core thus rendering the envelope with the observed solar composition.

(ii) *Enhanced Angular Momentum Braking of the Central Grains*

The second feature which we may deduce from Equation (19) is that by the time the predominantly solid H_2 grains have condensed out, at time $t = t_0$ say, and collapsed to radius $S_1 \sim 0.1$ at time $t_0 + t_c$, given by Equation (18), the early forming and fast moving grains which consist predominantly of C, N, O ices which condensed at time $t = 0$, say, will have already collapsed to a distance S_2 which may be very much smaller than S_1. Indeed we have

$$S_2 = \exp\left[-\frac{k^2}{\langle\gamma\rangle}(t_0 + t_c)\frac{\rho_s a}{\langle\rho_s a\rangle}\right] \simeq 0.01, \tag{20}$$

taking $t_0 = t_c$, $\rho_s a \sim 10\langle\rho_s a\rangle$ as typical values. For a grain of average composition ($X = 0.7$, $Y = 0.28$, $Z = 0.02$) we have $\langle\rho_s\rangle \simeq 0.11$.

From Equation (20) it follows that not only will the concentration of metal-rich and very fast moving grains be enhanced at the centre of the cloud, as we saw before, but in addition these fast grains will also give up virtually all of their initial angular momentum per unit mass l_i. Indeed, since these grains fall with uniform angular velocity ω_0, given by Equation (12) we have $l_2 = l_i S_2^2 \simeq 10^{-4} l_i$. Hence these grains will give up 4 orders of magnitude of their angular momentum and so by Section 2.1 may later be able to safely collapse to stellar size without threat of rotational disruption. Since metal-rich grains make up at most 2% of the fractional mass of the cloud, if they consist solely of CNO, whilst exceptionally large solid H_2 grains may perhaps make up a further few per cent we see that perhaps as much as 5% of the original grain cloud mass is able to give up most of its angular momentum in this way. For the remainder of the cloud, which on the average is able to collapse only to radius $S_1 \sim 0.1$ before sweeping up the gases of the cloud, only two orders of magnitude of angular momentum can be lost. The final angular momentum of the cloud is still therefore much the same as before, viz., $L_f = L_i S_1^2 \simeq 1 \times 10^{52}\ \mathrm{g\,cm^2\,s^{-1}}$.

3. Stabilization of the Collapsing Proto-Stellar Cloud

3.1. Introduction

When all grain braking has ceased the grain cloud and imprisoned neutral gases commence to fall freely. The calculations of Penston (1966), Bodenheimer and Sweigart (1968), Disney *et al.* (1969), and Larson (1969) suggest that the collapse from this point should occur nearly isothermally but extremely non-homologously. The density profile of the cloud progressively increases inwards becoming sharply peaked towards the centre. When the central density of the cloud approaches $10^{-13}\mathrm{g\,cm^{-3}}$ corresponding to a radius of $\sim 2 \times 10^4 R_\odot$ for a uniform cloud of solar mass, the material at the centre becomes opaque to the transmission of infrared radiation. The central regions then begin to heat up as the gravitational energy released in the collapse becomes unable to escape freely.

The heat generated in the centre in this way is more than ample to melt all of the ice-like grains in the remainder of the cloud.

The temperature and density at the centre continue to increase nearly adiabatically until the collapse of the central region is halted. During adiabatic contraction the pressure $p \propto \rho^{\gamma}$ increases as $R_c^{-3\gamma}$, where γ here is the ratio of specific heats and R_c the radius of the central region. Since the gas pressure $(\rho \mathscr{R} T/\mu)_c$ required for hydrostatic equilibrium changes only as R^{-4} we see that the collapse is halted as long as $\gamma > 4/3$. As soon as the central temperature rises to 2000 K, however, dissociation of the molecular hydrogen sets in followed by ionization of atomic hydrogen and helium, causing γ to fall below 4/3. Larson finds that a small fraction of $\sim 1\%$ of the cloud mass falls all the way through to stellar size long before the remainder of the cloud has collapsed to $\sim 10^4 R_\odot$.

The possibility that supersonic turbulence may stabilize the collapse of the infalling cloud has been suggested by Schatzman (1967). If the turbulent pressure is sufficiently great it is in principle possible for the effective γ of the cloud to be kept above 4/3, so that the whole cloud may exist in a Kelvin-Helmholtz hydrostatic equilibrium during the contraction of radius from $10^4 R_\odot$ to $10^2 R_\odot$. A reconsideration of this matter by Schatzman (1971) shows, however, that when one equates the convective heat transfer rate with the energy release rate during gravitational contraction, the convective velocities never become large enough to create a turbulence strong enough to stabilize the cloud.

Schatzman's 1971 calculation is based on the conventional mixing-length theory of convection. Recently, Prentice (1976) has questioned the validity of one of the basic premises of this theory, namely the premise that the convective elements always thermalize themselves inside the convective layer. If in a strongly convective unstable zone the mixing-length λ is comparable with the thickness of the zone then it is possible for an eddy originating at some point in the unstable zone and moving nearly adiabatically to overshoot into the surrounding radiatively stable layers to a point where the entropy of the eddy and the average surroundings are the same, and thence to decelerate to rest beyond this point under the action of negative buoyancy before returning, again nearly adiabatically, to its starting point in the form of a stable return flow, without having mixed with the surroundings. That is, in the case of a strongly convectively unstable star, where the mean temperature gradient is strongly superadiabatic, we cannot preclude the possibility that there may exist a reservoir of nearly adiabatic mechanical motions. The convective heat flux in this instance depends on the temperature difference between the eddy and its stable return flow and this can be made quite small, as in the conventional mixing-length theory, as long as the motions are nearly adiabatic, even though the driving buoyancy force which depends on the temperature difference between the eddy and the average stationary surroundings may be quite large. Viscous and supersonic shock-wave losses which might affect the adiabaticity of the convective motions are rendered unimportant if the eddies are long and needle-like (Prentice, 1973). In addition, the assumption of negligible thermal mixing is valid in this model since the radiative adjustment time of the convective element is many times longer than the buoyant rise time.

In the case of a fully convective star, the upper overshoot zone lies above the photosurface. Since there is no lower overshoot zone, however, we cannot construct a reservoir of downward originating convective elements in such a star. The motions of the negatively buoyant elements are, therefore, quenched at the centre and probably can be neglected. That is, most of the turbulent stress in the star is due to the positively buoyant rising elements.

Prentice (1973) has shown that the radial turbulent stress P_t arising from the buoyancy driven eddy motions is given by

$$P_t = \beta\rho GM(r)/r, \quad \beta = \tfrac{2}{3} f_t k |1 - \psi|, \tag{21}$$

where β is called the turbulence parameter, assumed to be a constant throughout the star, $M(r)$ is the mass interior to radius r, f_t is the mean mass fraction of moving eddy material, $k = \lambda/r$ the ratio of the mean eddy acceleration-length λ to local radius r, and $|1 - \psi| = \langle|\Delta T|/T\rangle$ is the mean temperature excess factor. In the normal mixing length theory of convection each of $k, f_t, |\psi - 1|$ is much less than unity so that $\beta \ll 0.1$. Nonetheless, if the convection is very strong, such as we suggest exists in the pre-Main Sequence phase of gravitational contraction, and overshooting of convective motions takes place, then it is possible as we have described above for β to become important. Typically we expect $k \sim 1, f_t \sim 0.5, |1 - \psi| \sim 0.2$ and hence $\beta \sim 0.1$. In addition, if the return flow motions contribute substantially to the total turbulent stress, Equation (21) for β is somewhat altered and β may become larger than unity (Prentice, 1976).

In this section therefore we shall reconsider in detail the possibility that supersonic turbulent convection may stabilize the collapse of the infalling protostellar cloud. We also include the influence of rotation and consider what additional influence the formation of a small central luminous core, along the lines pursued by Larson (1969), may have in halting the collapse of the cloud.

3.2. THE INFLUENCE OF SUPERSONIC TURBULENT CONVECTON – NO CENTRAL CORE

The free collapse of the infalling protostellar cloud is halted as soon as sufficient energy is supplied to dissociate and ionize the hydrogen and helium gas to the levels required for both thermodynamic and hydrostatic equilibrium. The total initial energy of the grain cloud, E_∞ say, is essentially zero. If we neglect for the moment the possible formation at the centre of the cloud of a small luminous core of stellar size, the total energy $E(R_e)$ of a uniformly rotating turbulent cloud of equatorial radius R_e existing in hydrostatic equilibrium is given by

$$E(R_e) = -\Omega_{\mathrm{grav}} + U_{\mathrm{th}} + U_{\mathrm{turb}} + U_{\mathrm{rot}} + \mathscr{E}, \tag{22}$$

where

$$\Omega_{\mathrm{grav}} = \iiint \frac{\rho GM(r)}{r}\, \mathrm{d}^3\mathbf{r} \equiv C_n(\beta, \Theta) GM^2/R_e \tag{23}$$

is the self-gravitational potential energy of the cloud, C_n being a concentration factor which we describe below, and

$$U_{\rm th} = \frac{1}{2}\iiint \nu\rho\frac{\mathscr{R}T}{\mu}\mathrm{d}^3\mathbf{r} \simeq \frac{1}{2}(1-3\beta)\Omega_{\rm grav}, \quad U_{\rm turb} = \frac{\beta}{2}\Omega_{\rm grav}, \tag{24}$$

are the thermal and turbulent kinetic energies of the gas and

$$U_{\rm rot} = \tfrac{1}{2}f\Theta GM^2/R_e \tag{25}$$

is the rotational energy where $\Theta = \omega^2 R_e^3/GM$ is the equatorial rotation parameter. In deriving Equations (24) we used the equation for hydrostatic support

$$\mathrm{d}p_{\rm tot}/\mathrm{d}r = -\rho GM(r)/r^2, \tag{26}$$

where

$$p_{\rm tot} = \rho\mathscr{R}T/\mu + \beta\rho GM(r)/r \tag{27}$$

is the total radial stress at radius r. In Equation (24) ν is the mean number of degrees of freedom per atom. This varies from 3 in the central regions of the cloud, which are completely dissociated and ionized, to a value $\nu_2 = 2n_2$ in the outer cool layers which are undissociated, where n_2 is defined below (Equation (36)). The final term in Equation (22) is the total dissociation-ionization energy (in c.g.s. units) given by

$$\mathscr{E} = 5.0\times 10^{11}\int \{(14.3x_{\rm H} + 30.1x_{\rm H^+})X + (11.8x_{\rm He^+} + 37.9x_{\rm He^{++}})Y\}\rho\mathrm{d}^3\mathbf{r}, \tag{28}$$

where $x_{\rm H_2}$, $x_{\rm H}$, $x_{\rm H^+}$, $x_{\rm He}$, $x_{\rm He^+}$, and $x_{\rm He^{++}}$ are the fractional concentrations of the elements H, He in their various states of dissociation and ionization satisfying the totality conditions

$$x_{\rm H_2} + x_{\rm H} + x_{\rm H^+} = 1, \quad x_{\rm He} + x_{\rm He^+} + x_{\rm He^{++}} = 1, \tag{29}$$

and X, Y are the total fractional abundances of H and He. The quantities $x_{\rm H}, \ldots$ depend on the local temperature and density and may be computed from the normal Saha equation (Allen, 1962, p. 34), using a simplified system of algebraic equations, while the molecular weight μ is given by

$$\mu^{-1} = \tfrac{1}{4}\{[2x_{\rm H_2} + 4x_{\rm H} + 8x_{\rm H^+}]X + [x_{\rm He} + 2x_{\rm He^+} + 3x_{\rm He^{++}}]Y\}. \tag{30}$$

The factor $C_n(\beta, \Theta)$ in Equation (23) may be called a concentration coefficient since it depends on how centrally condensed the protostellar cloud is. It depends both on the turbulence parameter β and the rotation parameter Θ as well as other implicit structural quantities such as the polytropic index n. In general, for a strongly centrally condensed structure which is uniformly rotating we have the approximate relation

$$C_n(\beta, \Theta) = (1+\Theta/2)C_n(\beta, 0). \tag{31}$$

This relation tells us that rotation enchances the apparent store of potential energy in a cloud of given equatorial radius R_e. This is because in a centrally condensed cloud only

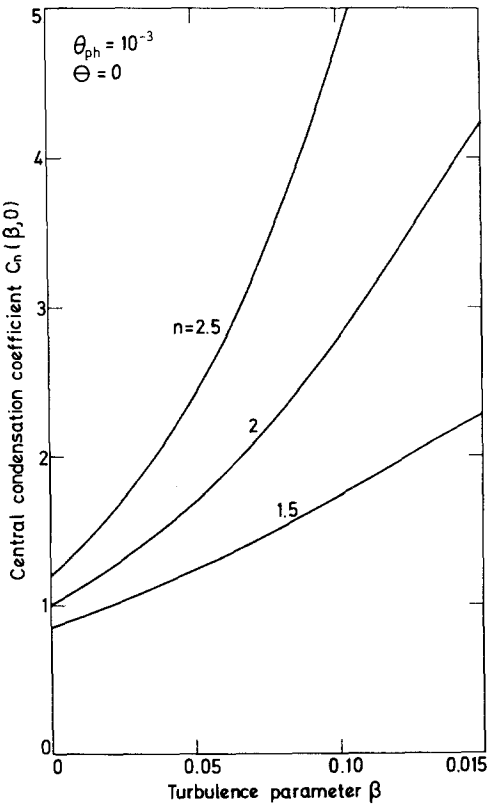

Fig. 1. The dimensionless gravitational potential energy measure, or central condensation coefficient, $C_n = \Omega_{\text{grav}}/(GM^2/R)$ of non-rotating turbulent polytropic structure of mass M and radius R, plotted against the turbulent parameter β for various polytropic indices n.

the outer layers are significantly disturbed by rotation, the equatorial radius exceeding the polar radius by the factor $R_e/R_p = 1 + \Theta/2$, whilst the central regions barely notice the centrifugal force. Rotation therefore has a stabilizing influence on a structure of given equatorial radius.

Figure 1 shows the variation of $C_n(\beta, 0)$ vs. β for adiabatic polytropic structures of uniform index $n = 1.5$ and 2.5 respectively, where the density ρ as a function of temperature T in adiabatic regions of varying molecular weight μ satisfies the relation

$$\rho \propto (T/\mu)^n. \tag{32}$$

Since the ratio of turbulent stress to gas pressure $P_t = \beta\mu GM/\mathscr{R}Tr$ becomes infinite when $T \to 0$ it is necessary to suppose, as in the case of a real star, that the surface of the star is defined by a non-zero photospheric temperature T_{ph}. We thus define

$$\theta_{\text{ph}} \equiv (T_{\text{ph}}/T_c)/(\mu_{\text{ph}}/\mu_c), \tag{33}$$

where T_c, μ_c are the central temperature and molecular weight and we have typically set $\theta_{\mathrm{ph}} = 10^{-3}$ in the calculations presented in Figure 1.

We observe that as the turbulence parameter β increases so does the concentration coefficient C_n, which means that the store of gravitational energy in a structure of given radius is increased by the turbulence. This behaviour is due to the fact that the turbulence is greatest in the outer less dense layers of the structure and causes these outer layers to be pushed outwards proportionately much more than the inner dense layers where the turbulent stress is small. Thus turbulence stress causes the star to become more centrally condensed. As $\beta \to 0$, C_n approaches the well-known limit

$$C_n(0, 0) \simeq 3/(5 - n), \tag{34}$$

appropriate to non-turbulent polytropic structures satisfying the zero surface temperature condition $\theta_{\mathrm{ph}} = 0$ (Cox and Giuli, 1968, p. 711). We see that turbulence can typically enchance C_n by a factor of 5 or so, whilst for a fully rotating star, rotation adds a further factor of 3/2.

Returning now to the question of hydrostatic equilibrium of the protostellar cloud, the free collapse from interstellar density can be halted as soon as $E(R_e) < E_\infty = 0$. The inequality applies here since some energy is radiated away from the surface during the collapse. Using Equation (22) we thus see that for stabilization we require that

$$\mathscr{E} \Big/ \left(\Omega_{\mathrm{grav}} - \sum_i U_i \right) \leqslant 1. \tag{35}$$

Figure 2 shows a plot of $\mathscr{E}/(\Omega_{\mathrm{grav}} - \Sigma_i U_i)$ against equatorial radius R_e for various degrees of turbulence β for the case $\theta_{\mathrm{ph}} = 10^{-3}$, $\Theta = 1$, and elemental abundance $X = 0.7$, $Y = 0.3$. It is supposed that the whole cloud exists in convective equilibrium and consists of two distinct polytropic layers. In the inner layer where the hydrogen is fully dissociated the polytropic index is $n_1 = 3/2$. In the outer layer, which extends to the surface, the hydrogen is largely molecular and the polytropic index n_2 is given by the equation (cf. Cox and Giuli, 1968)

$$n_2 = 3/2 + 2X/(1 + X) \tag{36}$$

Thus if the outer layer consists solely of hydrogen, so $X = 1$, then $n_2 = 2.5$ as expected.

Additional variations of n occur as a result of the spatial gradients in the levels of ionization and dissociation. If, however, the transition from one excitation state to the next occurs over a distance which is small compared to the physical radius of the star, then this source of variation should not have any significant influence on the overall structure of the star. For the sake of simplicity we shall assume that these transitions occur abruptly and concentrate our attention on the change in n due to the dissociation, which we have described above, for which n does not return to the same value, namely 3/2, once the dissociation zone has been crossed. The position of this zone in the star is computed from the condition that concentrations x_{H}, x_{H_2} of the species H, H_2 coincide at the interface of the n_1, n_2 polytropic layers.

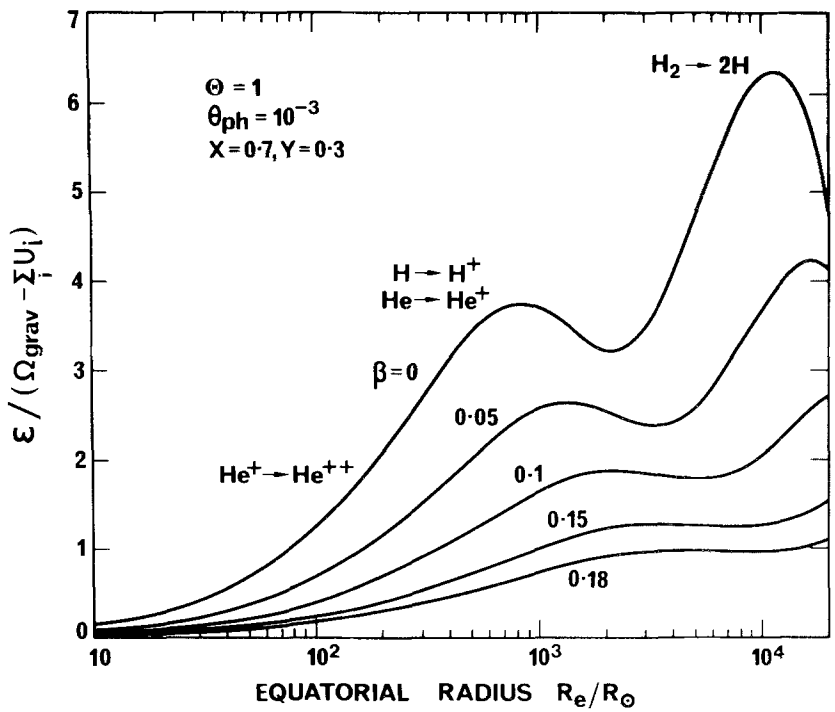

Fig. 2. Ratio of total dissociation and ionization energy $\mathscr{E}$ of a fully rotating turbulent protosolar envelope to available excess gravitational potential energy $\{\Omega_{\text{grav}} - \Sigma_i U_i\}$ plotted as a function of equatorial radius R_e for different cases of the turbulence parameter β where $\Sigma_i U_i$ is the sum of the thermal, turbulent and kinetic energies.

We observe from Figure 2 that supersonic turbulence helps to stabilize the infalling cloud. As β is increased the proportion of the residual potential energy $\Omega_{\text{grav}} - \Sigma_i U_i$ which is needed to dissociate and ionize the gases of the cloud to the levels required for complete thermodynamic equilibrium is reduced. Schatzman (1967) has suggested that supersonic turbulence may completely stabilize the protostellar cloud in the region of the present planetary system. Unfortunately, for a complete halt in the collapse we require $\mathscr{E}/(\Omega_{\text{grav}} - \Sigma_i U_i) \leqslant 1$ and we note from the diagram that this condition is nowhere met during the collapse from $10^4 R_\odot$ to $10^2 R_\odot$, except for most extreme instances where $\beta \geqslant 0.2$. For such large values of β the physical characteristics of the cloud assume absurdly extreme values. More to the point, we find later on that the values of β which are required to account for the physical properties of the planetary system, such as the Titius-Bode law and the distribution of planetary masses, are typically of order of only 0.1.

We therefore are led to conclude that supersonic turbulent convection is probably unable completely to stabilize the cloud during the collapse from a radius of $\sim 10^4 R_\odot$, though the modification to the mixing-length theory of convection which we mentioned in Section 3.1 above certainly greatly helps towards the achievement of this end.

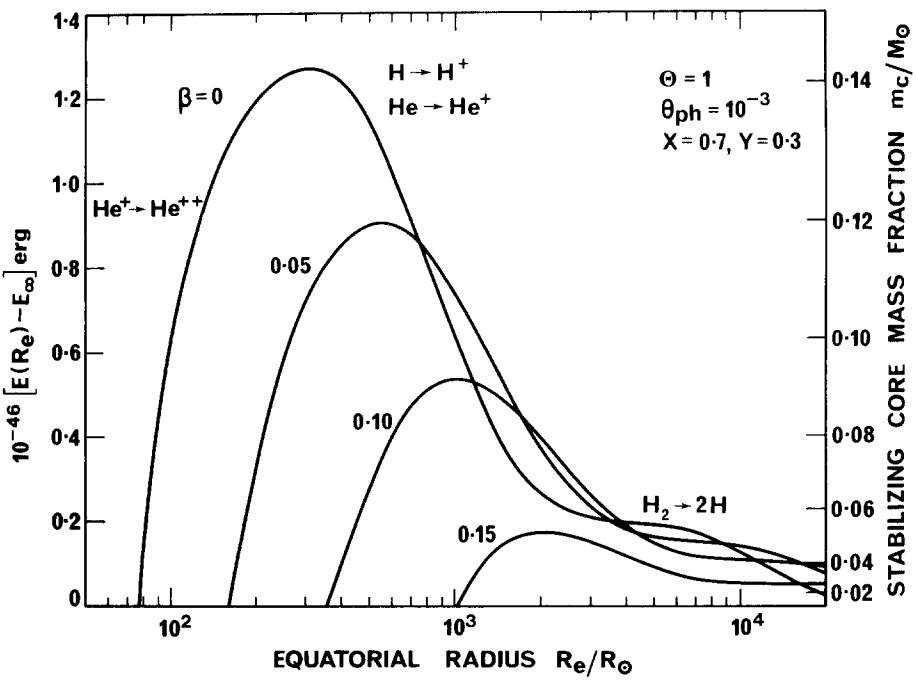

Fig. 3. Total energy $E(R_e)$ of the fully rotating turbulent protosolar envelope when existing in the state of complete hydrostatic and thermodynamic equilibrium at equatorial radius R_e, in units of $R_\odot$, where $E_\infty = 0$ is the energy at infinite radius. To achieve a consistent equilibrium first at radius $10^4 R_\odot$ we see that a small fraction $m_c = 3$–$4\% M_\odot$ of the central region of the envelope need collapse to stellar size liberating sufficient energy $Gm_c^2/2r_c = E(R_e) - E_\infty$ to stabilize the rest of the envelope.

3.3. Formation of a Small Central Luminous Core

In Figure 3 we have plotted the additional amount of energy $E(R_e) - E_\infty$ which is required to achieve hydrostatic equilibrium throughout the fully rotating turbulent proto-stellar clouds discussed above in Figure 2, for various values of the turbulence parameter β and as function of the equatorial radius R_e. We see that in the absence of any additional source of energy, no complete thermodynamic equilibrium can be attained until the radius has typically shrunk to the value $\sim 300 R_\odot$, corresponding to the present orbit of Venus, for the case $\beta = 0.1$. The cloud is therefore dynamically unstable in the interval $10^4 R_\odot$ to $300 R_\odot$ and will proceed to collapse freely. Nevertheless, since the free fall time τ_{ff} at any point in the cloud varies as $\tau_{ff} \propto 1/\sqrt{G\bar{\rho}(r)}$, where $\bar{\rho}(r)$ is the mean mass density interior to radius r, it follows that the central regions of the cloud will reach the centre sooner than the outer ones since $\bar{\rho}(r)$ is a centrally peaked function whether one considers a cloud in free fall (Larson, 1969) or a cloud existing in supersonic convective equilibrium (Prentice, 1973).

We therefore propose that a small fraction of mass m_c of the central region of the cloud collapses dynamically all the way through to stellar size, to a radius r_c say, where

the hydrostatic temperature exceeds both the dissociation and ionization temperatures, and where the gravitational energy released is sufficient to stabilize the rest of the infalling cloud. The energy released through the formation of such a small central core is

$$\frac{1}{2}\frac{Gm_c^2}{r_c} = 1.9 \times 10^{48}\left(\frac{m_c}{M_\odot}\right)^2\frac{R_\odot}{r_c}\text{erg}. \tag{37}$$

If all of this energy is absorbed by the remainder of the infalling cloud, the amount of material which must collect at the centre to achieve a complete stabilization is seen to be

$$\frac{m_c}{M_\odot} = 1.26 \times 10^{-24}\,[E(R_e) - E_\infty]^{1/2}, \tag{38}$$

if we set $r_c = 3R_\odot$.

We have shown the required mass $m_c/M_\odot$ along the ordinate on the right hand side of Figure 3. We see that for all values of β typically in the range 0 to 0.15, we initially require a central core mass fraction ~ 2–$4\%M_\odot$ to accumulate at the centre to stabilize the infalling cloud when it first becomes sufficiently opaque to absorb the emitted radiation near a radius of $\sim 10^4 R_\odot$. Thus the inner few per cent of the cloud mass never achieve any equilibrium until they reach normal stellar size and so remain detached from the rest of the protostellar cloud during the latter's pre-Main-Sequence contraction. Any metal-rich central inhomogeneity which was formed at the end of the grain braking era, described in Section 2.4, may therefore survive the turbulent era of planetary formation, when the rest of the low density ($10^{-13}\,\text{g cm}^{-3}$) cloud is uniformly mixed up by the supersonic convection. Therefore, when the protosolar cloud finally moves onto the zero-age Main Sequence it probably consists of a small metal-rich central core, of mass as much as $0.04M_\odot$, surrounded by a homogeneous envelope of normal composition. Prentice (1976) has recently drawn attention to the importance of this result in being able to account for the observed present low solar neutrino flux, as well as various other astronomical and geophysical anomalies.

3.4. The Influence of Rotation

We should point out that the centrifugal force will not prevent the formation of the small central stabilizing core from taking place since we found earlier, in Section 2.4, that the inner 5% or so of the grain cloud have virtually zero angular momentum at the end of the grain-braking era. In addition, as soon as the infalling cloud has been stabilized, turbulent viscosity (see Section 4) tends to eliminate any differential rotation which may have developed in the cloud during its free collapse. This means that if the protostellar cloud becomes destabilized again, further material from the central regions of the cloud is able to safely collapse to stellar radius, to stabilize the structure again, without the threat of rotational disruption. To appreciate this point let us note that the rotation parameter $\Theta(x)$ of a point in the equatorial plane at fractional radius x and fractional mass point $q(x)$ from the centre inside a uniformly rotating cloud having equatorial rotation parameter Θ_1 is given by the equation

$$\Theta(x) = \Theta_1 x^4/q(x). \tag{39}$$

For a very centrally condensed cloud, at least 10% of the mass typically resides within 10% of the equatorial radius so that $\Theta(0.1) \leqslant 10^{-3}\Theta_1$. This means that even for a fully rotating cloud ($\Theta(1) = 1$) the inner 10% of the mass is able safely to reduce its radius by more than a factor of 1000 before centrifugal forces become important. Thus, once the cloud has become initially stabilized near a radius of $\sim 10^4 R_\odot$, further growth of the central core of radius $r_c \sim 3 R_\odot$ will not be prevented by rotational forces.

3.5. Rate of Collapse of the Proto-Stellar Cloud

We may suppose that as soon as the cloud has become stabilized at a radius near $\sim 10^4 R_\odot$ it proceeds inwards over a Kelvin-Helmholtz time-scale. However, as the cloud contracts we see from Figure 3 that it immediately becomes destabilized again as further energy is required to complete the dissociation and ionization processes to the level required for complete equilibrium. The central regions of the cloud proceed to collapse inwards again releasing more energy as they fall onto the central embryonic core and thereby restabilizing the cloud. This quasistatic state persists until the maximum of the $E(R_e) - E_\infty$ function has been passed, near radius $\sim 1000 R_\odot$. The cloud therefore exists in a state of quasistatic equilibrium during the interval when it collapses from $\sim 10^4 R_\odot$ to $\sim 10^3 R_\odot$, with the rate of collapse at the surface being governed by the rate of accumulation of material at the centre. Once the maximum point of $E(R_e)$ has been passed the collapse proceeds at the normal Kelvin-Helmholtz rate. If we let v_e denote the inward radial velocity at the equator then we have

$$\begin{aligned} v_e &= \left[L_{\mathrm{rad}} - \frac{G m_c \dot{m}_c}{r_c} H\left(-\frac{\mathrm{d}E}{\mathrm{d}R_e}\right)\right] \Big/ \frac{\mathrm{d}E(R_e)}{\mathrm{d}R_e}, \\ L_{\mathrm{rad}} &= 2.82\,\pi\sigma_s R_e{}^2 T_e^4 , \end{aligned} \tag{40}$$

where the factor 2.82π refers to the surface area of a fully rotating centrally condensed structure of unit equatorial radius, L_{rad} is the surface luminosity and $H(x)$ is the Heaviside function.

If the material which accumulates at the centre falls freely from radius r_1 in the cloud where the density is ρ_1 and $r_c \leqslant r_1 \ll R_e$, then we have $\dot{m}_c = 4\pi\rho_1 r_1{}^2 b\sqrt{G m_c/r_1}$ where b is a number of order unity. The ratio of v_e to the free fall speed $v_{ff} = \sqrt{GM/R_e}$ at the equator then becomes, for the region $\mathrm{d}E/\mathrm{d}R_e < 0$, on neglect of L_{rad},

$$\frac{v_e}{v_{ff}} \simeq \left(\frac{m_c}{M}\right)^{3/2} \frac{GM^2/R_e^2}{\mathrm{d}E/\mathrm{d}R_e}\left[\frac{3\rho_1}{\bar{\rho}} b\left(\frac{r_1}{R_e}\right)^{3/2}\frac{R_e}{r_c}\right], \tag{41}$$

where $\bar{\rho}$ is the mean density of the cloud. Inserting typical values $GM^2/R_e^2 \sim \mathrm{d}E/\mathrm{d}R_e$, $\rho_1/\bar{\rho} \sim 10^2$–$10^3$, $b \sim 0.1$–1, $r_1 \sim r_c \sim (10^{-4}$–$10^{-3}) R_e$ we obtain

$$\frac{v_e}{v_{ff}} = O\left[\left(\frac{m_c}{M}\right)^{3/2}\right] \sim 0.01\text{–}0.03, \tag{42}$$

taking $m_c/M_\odot = 0.03$–0.1. Thus, roughly speaking, during the period of quasistatic equilibrium, the rate of collapse at the surface of the cloud lies somewhere between 1/100th and 1/10th of the free fall rate. Once the cloud has become fully stabilized near a radius of $\sim 10^3 R_\odot$ the collapse proceeds much more slowly as we have indicated in the Table II using representative surface temperatures and taking $E(R_e) \simeq -GM^2/R_e$. The local collapse time $\tau_c = R_e/v_e$ is indicated in the table as well as the mode of equilibrium.

We see that the collapse from $10^4 R_\odot$ to $10^3 R_\odot$ is very rapid in comparison to the collapse from $10^3 R_\odot$ to $10 R_\odot$, which takes some 2×10^5 yr to complete. A more detailed computation of the collapse rate appears in Section 7.

TABLE II

Contraction rate of the proto-solar envelope

$R_e(R_\odot)$	10	10^2	10^3	10^3	3×10^3	10^4
T_e (K)	4000	1000	150	150	50	20
v_e/v_{ff}	8×10^{-9}	1×10^{-6}	2×10^{-5}	0.01	0.01	0.01
τ_c (yr)	2×10^5	5×10^4	1×10^5	150	800	5000
mode	K–H	K–H	K–H	*QS*	*QS*	*QS*

4. Physical Structure of the Turbulent Rotating Proto-Sun

4.1. INTRODUCTION

In this section we shall examine the physical structure of the turbulent rotating protosun after it has become energetically stabilized near a radius of $\sim 10^4 R_\odot$. We shall not be concerned so much with the details of the structure at the centre, where the presence of a compact central core of stellar radius induces a fairly complex hydrodynamic inflow during the period of core growth, but rather with the details of the density and pressure profiles near the surface of the cloud where, apart from rotation and convective turbulence, the material exists in quasi-static equilibrium. We consider the relative importance of rotation, turbulent stress, and magnetic forces on the static configuration of the protosolar cloud, or protosun, but shall not at the moment study the evolutionary aspects of the contraction process where the conservation of total angular momentum induces profound changes near the surface of the cloud as it collapses through the dimensions of the present planetary system.

4.2. THE IMPORTANCE OF MAGNETIC FORCES

We saw in Section 2 that the ratio of magnetic to gravitational energies in the original extended interstellar cloud of radius 0.7 pc was $(U_{\text{mag}}/\Omega_{\text{grav}})_i = (10\pi/9\mu_0)B_i^2 R_i^4/GM^2 \sim 200$. We also saw how as a result of grain cloud formation at radius ~ 0.1 pc the main part of the gas was able effectively to isolate itself from the magnetic field by existing in solid form. In this way magnetic flux freezing is avoided until the cloud becomes so compressed that it begins to sweep up the ionic component of the residual gas cloud.

Prentice and ter Haar (1971) showed that such an event should not occur until the fractional radius of the grain cloud has shrunk to the value $S_{\rm ion} \sim 10^{-3}$. The final ratio of magnetic to gravitational energy in the cloud at that stage is then

$$(U_{\rm mag}/\Omega_{\rm grav})_f = S_{\rm ion}^4 (U_{\rm mag}/\Omega_{\rm grav})_i \sim 2 \times 10^{-10}, \tag{43}$$

which is neglibible. Since both the magnetic and gravitational energies increase at the same rate ($\propto 1/R$) during the subsequent collapse, it follows that the magnetic energy always remains unimportant relative to the gravitational energy and so may be safely ignored. More importantly it means, contrary to the starting point of some other workers (Hoyle, 1960; Alfvén and Arrhenius, 1973), that magnetic forces probably had very little influence on the structure and dynamical evolution of the proto-solar nebula during the fairly rapid contraction phase from radius $10^4 R_\odot$ to $2 R_\odot$. Of course, we have shown that magnetic forces do play a vital role during the very early stages of the Sun's formation, in the regime of interstellar densities. It is also possible that they play an important role during the long slow final phase of the Sun's pre-Main Sequence contraction, from radius $2 R_\odot$ down to $R_\odot$, when the interaction of the solar wind with a strong primordial magnetic field is required to rid the proto-Sun of the last vestige of its rapid rotation (Weber and Davis, 1967). During the brief period of planetary formation, however, which takes only some 3×10^5 yr to complete (see Section 7), we feel that magnetic forces can be safely ignored.

It is interesting to note that the magnetic field which we compute for the early sun of solar radius $R_\odot$ is $B_\odot \sim 3 \times 10^3$ G. This value is consistent with the maximum field strength of 3.5×10^4 G observed for very strongly magnetic stars. It also coincides rather closely with the magnetic field needed to account for the remnant magnetization of some lunar samples (Freeman, 1978).

4.3. Turbulent Stress and Turbulent Viscosity – No Rotation

As soon as the cloud has become sufficiently opaque to acquire a quasistatic convective equilibrium we suppose that the gravitational energy $[GM(r)/r^2]\, v_r$ released per sec at each mass point during the subsequent contraction is sufficient to drive a supersonic turbulence. When the convective elements or eddies are long and needle-like they experience very little drag passing through the gas and the turbulence stress p_t and total stress $p_{\rm tot}$ arising from these motions is given by Equations (21) and (27). The temperature and density for an adiabatic convective equilibrium are related by Equation (32), where $n = 1/(\gamma - 1)$.

(i) *The Moment-of-Inertia Coefficient f*

Prentice (1973) has shown, as mentioned earlier, that the main influence of the turbulent stress is to cause the cloud to become much more centrally condensed. This is because the turbulent stress exerts its greatest influence on the tenuous cool outer layers of the structure, pushing them greatly outwards and thereby lowering the so-called moment-of-inertia coefficient f defined by

$$I = MR_e{}^2 f, \tag{44}$$

where I is the moment of inertia about the rotational axis and R_e the equatorial radius. For a non-rotating polytrope of index $n = 1.5$, f is typically reduced from 0.205 to 0.045 as β passes from 0 to 0.15. For a polytrope of index 2.5 the reduction is from 0.112 to 0.007 as β goes from 0 to 0.15. These values depend fairly weakly on the chosen value of the photospheric temperature ratio $\theta_{\rm ph}$, defined by Equation (33), as well as β for $\beta \gtrsim 0.1$. Typically $\theta_{\rm ph} = 10^{-3}$. As β increases from 0 so does the ratio of turbulent stress to gas pressure just beneath the photosphere. For all $\beta \geqslant 0.01$, this ratio rises very quickly to a plateau level given by

$$P_{\rm ph} = \frac{\beta \mu GM}{\mathscr{R} T_{\rm ph} R_e} \sim 100, \tag{45}$$

taking $n = 1.5, \theta_{\rm ph} = 10^{-3}$.

(ii) *Photospheric Density Inversion*

A second main influence of turbulent stress on the structure of the cloud is the formation of a very steep density inversion at the visible surface or photosphere. If the turbulent convection dies down above the photosphere over an overshoot height which is at most a few pressure scale heights $H_{\rm ph}$, given by

$$H_{\rm ph} = \frac{\mathscr{R} T_{\rm ph} R_e^2}{\mu GM} = \beta R_e / P_{\rm ph} \simeq 10^{-3} R_e, \tag{46}$$

then overall pressure equilibrium demands that the density ρ_e at the base of the non-turbulent atmosphere just above this point exceed the density $\rho_{\rm ph}$ just beneath the photosphere by the factor

$$\rho_e / \rho_{\rm ph} = 1 + P_{\rm ph} \sim 100. \tag{47}$$

In view of the fact that $H_{\rm ph} \ll R_e$ we see that the density inversion occurs almost discontinuously with respect to the cloud radius variable R_e.

Beyond the photosurface where the radiation from the interior of the cloud is at last able freely to radiate away, the temperature is nearly a constant but the density decreases rapidly according to the equation

$$\rho(r) \underset{r \geqslant R_e}{=} \rho_e \exp\left[-(r - R_e)/H_{\rm ph}\right], \quad T(r) \simeq T_{\rm ph}. \tag{48}$$

The outermost layer of the young convective structure thus consists of a very dense but very thin shell of essentially non-turbulent gas. The mass of this non-turbulent outer shell is

$$m_{\rm sh} = 4\pi \rho_e R_e^2 H_{\rm ph}. \tag{49}$$

(iii) *Turbulent Viscosity*

The rising and falling supersonic convective motions create at each point in the cloud a turbulent viscosity given by

$$\eta_{\text{turb}} = \tfrac{1}{3}\rho_t v_t \lambda = \tfrac{1}{3} k f_t^{1/2} \beta^{1/2} \rho [GM(r)r]^{1/2}. \tag{50}$$

This viscosity eliminates differential motions and rotations in the cloud over a time-scale

$$\tau_{\text{turb}} = \rho r^2/\eta_t = (3/k f_t^{1/2} \beta^{1/2})[r^3/GM(r)]^{1/2}, \tag{51}$$

which is one of the same order as the local free-fall time $\tau_{ff} = [r^3/GM(r)]^{1/2}$. Physically therefore this means that as long as the rate of collapse of the cloud occurs at a slower rate than the free-fall rate, then the supersonic turbulence is able to remove any differential motions generated in the interior by the collapse. In short this means that the cloud is able to preserve its density profile and, in the case of a rotating cloud, to maintain uniform angular velocity throughout the interior.

To appreciate this point more precisely let us note that during quasi-static collapse of a fully rotating star each unit mass near the equator experiences an inertial azimuthal torque $\frac{1}{2} v_r (GM/r)^{1/2}$, where v_r is the radial inflow velocity at the equator. This torque tends to set up a differential azimuthal velocity field $v_\phi \propto (GM/r)^{1/2}$ which is eliminated by the viscous torque per unit mass $\eta_{\text{turb}} v_\phi / \rho r$, if we use Equation (21), provided

$$v_r/v_{ff} \lesssim \beta \sqrt{\frac{2}{3} \frac{k}{|1-\psi|}} \sim 0.1\text{–}0.3, \tag{52}$$

where $v_{ff} = (GM/r)^{1/2}$ is the free-fall velocity, taking typical values for β, $k \sim 1$, and $|1 - \psi|$. Now comparing Equations (42) and (52) we see that the requirement for uniform convective equilibrium in the rotating cloud will almost certainly be satisfied by the cloud during the collapse from radius $10^4 R_\odot$ to $10^3 R_\odot$ and will be more than adequately satisfied below this point when $v_r \simeq v_{\text{KH}}$ and $v_{\text{KH}}/v_{ff} \ll 1$.

Thus we may conclude that during the collapse of the proto-solar cloud through the dimensions of the planetary system, the supersonic turbulent stress maintains uniform rotation and an equilibrium density-profile throughout the convective structure. In this case the rotational state of the cloud is meaningfully defined by the single equatorial rotation parameter

$$\Theta \equiv \Theta_e = \omega_e^2 R_e^3/GM, \tag{53}$$

where ω_e is the angular velocity at the equator.

4.4. Influence of the Rotation on the Internal Structure of the Proto-Solar Cloud

It is well-known (cf. Jeans, 1928; p. 245) that as the rotation parameter Θ passes from 0 to 1 the various equipotential surfaces in the cloud become distorted from sphericity and bulge outwards at the equator. If, however, the cloud is strongly centrally condensed, meaning that the moment-of-inertia coefficient $f \ll 1$, then only the outermost layers are

significantly disturbed by the rotation and the so-called atmospheric approximation may be employed to compute the equilibrium structure of the outer layers. According to this approximation, the mass $M(r)$ interior to any radius r in the outer layers satisfies the equation

$$M(r) \simeq M = \text{constant},$$

and the equation of hydrostatic support may be written as

$$\frac{1}{\rho}\nabla p(s, z) = -\frac{GM}{R_e^2}\left\{\frac{R_e^2}{r^2}\hat{\mathbf{r}} - \Theta\frac{s}{R_e}\hat{\mathbf{s}}\right\}, \tag{54}$$

where s, z are cylindrical polar coordinates referred to the axis of rotation and $p = p(s, z)$ the total pressure, whilst $r = \sqrt{s^2 + z^2}$. If the equipotential surfaces of the various physical quantities $p, \rho, T/\mu$ everywhere coincide, then the solution of equation (54) may be formally written as

$$p = p(\Psi), \quad \rho = \rho(\Psi), \quad T/\mu = F(\Psi), \tag{55}$$

where the equipotential function $\Psi = \Psi(s, z)$ is given by

$$\Psi(s, z) = \left(\frac{3}{2 + \Theta}\right)\left[\frac{R_e}{r} - 1 + \frac{1}{2}\Theta\left(\frac{s^2}{R_e^2} - 1\right)\right]. \tag{56}$$

The photosurface is defined by the equation

$$\Psi(s, z) = 0. \tag{57}$$

The above equations allow us to compute the equipotential surfaces of the rotating cloud in terms of those of the spherical non-rotating cloud ($\Theta = 0$). Since the polar radius R_p of a very centrally condensed cloud is hardly affected by rotation (Monaghan and Roxburgh, 1965) it follows from Equation (56) that, as Θ is increased, the equatorial radius R_e increases according as

$$R_e(\Theta) = R_e(0)[1 + \Theta/2], \tag{58}$$

whilst the moment-of-intertia coefficeint $f(\Theta)$ declines according to the law

$$f(\Theta) \simeq f(0)[R_e(0)/R_e(\Theta)]^2 = f(0)/[1 + \Theta/2]^2. \tag{59}$$

Thus as Θ is increased from 0 to 1, the equatorial radius increases by 50% whilst the f is reduced by a factor 4/9. For the case of the turbulent polytropes of index $n = 1.5$, rotation reduces f from 0.045 to 0.020 for the typical case $\beta = 0.15$, $\theta_{\text{ph}} = 10^{-3}$. Since for the non-rotating non-turbulent cloud $\beta = 0$, $\Theta = 0$ we have $f = 0.205$ we see how the combination of supersonic turbulence and rotation can drastically reduce f by more than one order of magnitude. Choosing a larger polytropic index $n = 2.5$ (corresponding to an undissociated H_2 cloud) causes f to fall to about 0.003 for the same value of θ_{ph} and $\beta = 0.15$ (Prentice, 1973). It is reasonable therefore to suppose that the moment-of-inertia coefficient of the young proto-solar cloud probably lay in the range

$$0.003 \leqslant f(1) \leqslant 0.02 \tag{60}$$

with 0.01 as a typical mean value.

4.5. THE EXISTENCE OF A DENSE EQUATORIAL RING

Above the photosurface of the cloud the material is essentially non-turbulent and therefore free of turbulent viscosity. We therefore certainly cannot assume that the outermost layers of the cloud necessarily co-rotate with the same angular velocity ω_e as the convective material beneath the photosurface. This is especially the case when material is transferred from the interior of the cloud during the period of quasi-static gravitational contraction, when the time scale is much too short for other dissipative processes such as small scale isotropic fluid turbulence to become important. Instead we assume that each new element emerging from inside the cloud will preserve its angular momentum ωs^2 per unit mass once it crosses the photosurface. Thus for material which moves parallel to the axis of rotation of the cloud we have $\omega = \omega_e$ but for material which streams away from the cloud in the equatorial plane, ω declines as $1/s^2$.

Assuming then that all of the material which makes up the non-turbulent outer layers of the cloud originates from the convective interior in this manner, a good approximation to the angular velocity distribution above the photosurface is given by

$$\omega(s, z) = \begin{cases} \omega_e & s \leqslant R_e; \\ \omega_e(R_e/s)^2, & \text{if} \quad s > R_e. \end{cases} \tag{61}$$

The different zones of the angular velocity distribution are shown in Figure 4. We note that ω is constant on cylindrical surfaces. We should also mention that the distribution is only to be regarded as an approximate one since the angular velocity ω_e of the convective interior changes slightly both when material is transferred from the deep interior under conditions of uniform rotation and since R_e itself changes with changing Θ. Nevertheless since these changes mean that the inverse square power index in Equation (61) is changed only to, say, -1.9 or -1.95 we shall not concern ourselves with this minor correction at the present stage (see Section 5).

Next, if we assume, as seems reasonable, that the temperature above the photosurface is sensibly uniform and equal to the value T_{ph} at the photosurface itself, so that

$$T(s, z) \simeq T_{\text{ph}}, \quad \Psi(s, z) < 0, \tag{62}$$

the equation of hydrostatic support in the non-turbulent outer shell becomes

$$\frac{\mathscr{R}T_{\text{ph}}}{\mu\rho}\nabla\rho = -\frac{GM}{r^2}\hat{\mathbf{r}} + \omega^2 s\hat{\mathbf{s}}, \quad p = \rho\mathscr{R}T_{\text{ph}}/\mu. \tag{63}$$

The solution of this equation for the density distribution then reads

$$\rho(s, z) = \rho_e \exp(\alpha(1)\Psi), \quad \Psi < 0, \tag{64}$$

where

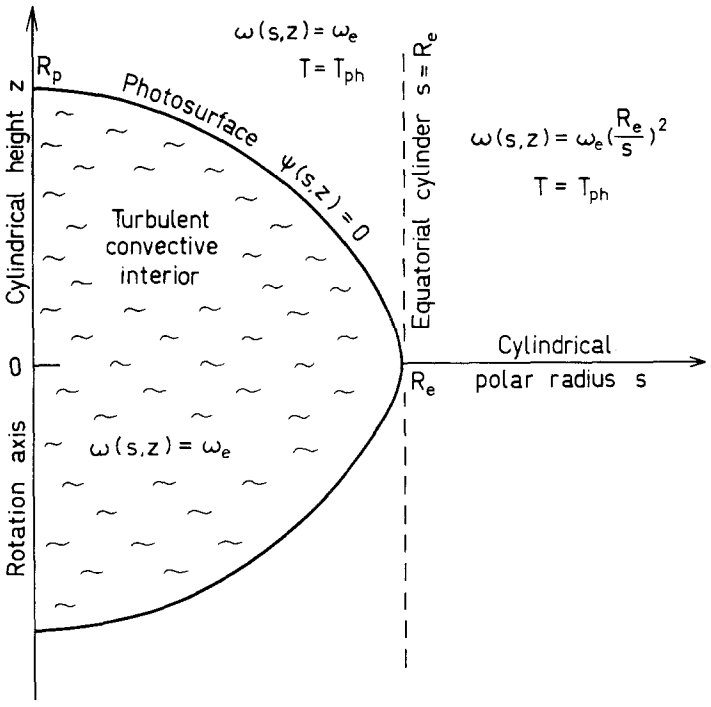

Fig. 4. Semi-polar cross-section of the turbulent rotating protosun showing the domain of the angular velocity distribution $\omega(s, z)$ of the gas described in terms of cylindrical polar co-ordinates (s, z), referred to the axis of rotation of the proto-Sun. The angular velocity at the equator is ω_e. The temperature outside the photosurface $\Psi(s, z) = 0$ is assumed to be a constant, namely $T_{\rm ph}$, which is the value at the photosurface.

$$\left(\frac{2+\Theta}{3}\right)\Psi(s, z) = \frac{R_e}{r} - 1 + \frac{1}{2}\Theta\begin{cases}[(s/R_e)^2 - 1], & \text{if} \quad s \leqslant R_e,\\ [1 - (R_e/s)^2], & \text{if} \quad s > R_e,\end{cases} \tag{65}$$

and

$$\alpha(\Theta) = \mu GM/\mathscr{R}T_e R_e(\Theta), \quad \alpha(0) = P_{\rm ph}/\beta, \tag{66}$$

where the photosurface stress ratio $P_{\rm ph}$ is given by Equation (45) and ρ_e, as before, is the density of non-turbulent gas at the base of the photosurface. It is a simple matter to show that Equation (65) simplifies to Equation (48) for the density profile of the non-rotating cloud when $\Theta \to 0$, whilst all the other physical quantities $T_{\rm ph}, P_{\rm ph}, \ldots$ have the same values as for the non-rotating cloud of the same polar radius R_p.

Figure 5 shows a meridional profile of some of the equipotential surfaces of the cloud for various degrees of rotation Θ which arise during the cloud's contraction from dimensionless polar radius $R_p/R_{p_0} = 1.6$ to 1, as we consider in Section 5. As R_p/R_{p_0} passes from 1.6 to 1, Θ increases from ~ 0.5 to 1. In each case the photosurface is defined by the curve $\Psi = 0$. We note, as Jeans (1928, p. 245) has also observed, that this surface

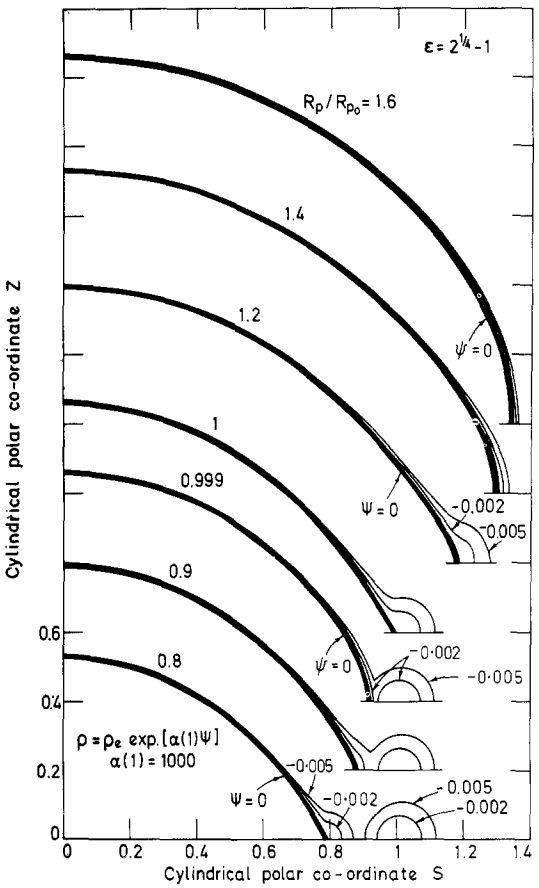

Fig. 5. Meridional cross-section of the equipotential surfaces $\Psi(s, z)$ of the outer layers of the protosolar envelope at various stages of the contraction, measured by the polar radius R_p, as the configuration approaches and passes through the first critical rotational point $R_p = R_{p_0}$ where the equatorial rotation parameter $\Theta_e = \omega^2 R_e^3/GM \to 1$. The photosurface ($\Psi = 0$) is indicated by the heavy line. A ring of gas is formed and left behind at cylindrical radius $s = 1 (R_e = R_0)$.

assumes a lenticular shape with a sharp edge at the equator as $\Theta \to 1$. The curves designated with $\Psi = -0.002, -0.005$ define the corresponding equipotential surfaces of the non-turbulent outer shell. We note with interest that as the rotation parameter is increased amongst this sequence of profiles that the originally spherical shell appears to evolve into an essentially ring-like structure at the equator. This phenomenon has remained unnoticed by earlier workers since it has always been loosely assumed that the non-turbulent atmosphere lying above the photosurface co-rotates with the interior of the cloud. Although this latter state of affairs may occur if the atmosphere persists with the cloud over a very long period of time, sufficient for a small-scale isotropic fluid turbulence to eliminate any differential motions, we certainly cannot assume this to be the case during the short period of gravitational contraction of the proto-stellar mass.

That is, the equatorial belt of gases owes its existence to the angular momentum distribution given by Equation (61) which expresses conservation of local angular momentum amongst material which originates freely from the cloud's interior.

(i) *Mass of the Equatorial Ring*

Expanding Equation (65) to second order in the local coordinates $\delta = s - R_e$ and z about the equatorial position $\delta = 0, z = 0$ we obtain for the density profile of the non-turbulent gases near the equator of the fully rotating cloud, the equation

$$\rho(s, z) = \rho_e \begin{cases} \exp\left[-\tfrac{1}{2}\alpha(1)(\delta^2 + z^2)/R_e^2\right], & s \geqslant R_e; \\ \exp\left[+\tfrac{1}{2}\alpha(1)(3\delta^2 - z^2)/R_e^2\right], & s < R_e. \end{cases} \tag{67}$$

The total mass of gas lying outside the equatorial cylinder $s = R_e$ is thus seen to be

$$m(1) = m_{\text{ring}} = 2\pi^2 \rho_e R_e^3(1)/\alpha(1) = 81\pi m_{\text{sh}}/32, \tag{68}$$

where m_{sh}, given by Equation (49), is the total mass of the non-turbulent spherical shell of the non-rotating star of the same polar radius R_p and turbulence parameter β as that of the rotating model.

The mass of the portion of the non-turbulent atmosphere which lies inside the equatorial cylinder is given approximately by

$$m_{\text{cyl}} \simeq \frac{\ln \alpha(1)}{\pi\sqrt{3}} m_{\text{ring}}. \tag{69}$$

In the typical situation for a turbulent polytrope of index $n = 1.5$ with $\theta_{\text{ph}} = 10^{-3}$, $\beta = 0.1$, $\Theta = 1$ we have $\alpha(1) = \frac{2}{3}P_{\text{ph}}/\beta \simeq 667$, using Equations (45), (66), and so $m_{\text{cyl}} \simeq 1.2 m_{\text{ring}}$. That means that almost half of the total non-turbulent atmosphere of the fully rotating cloud resides in the equatorial belt or ring outside the cylinder $s = R_e$. From Equation (68) we see that the mass of the ring itself exceeds that of the whole outer shell of the non-rotating model by a factor of nearly 8.

We conclude that not only does rotation cause the originally spherical shell of the non-rotating cloud to evolve into an essentially ring-like structure whose mass resides mostly beyond the equator, but the total mass of non-turbulent material which can be supported above the photosurface is also greatly enhanced.

5. Rotational Evolution of the Proto-Sun Towards the Point of Rotational Instability

5.1. Requirement for a Laplacian Hypothesis

We are now in a position to study the rotational evolution of the proto-Sun as it slowly collapses towards the point of rotational instability at radius R_0 given by

$$L_f \simeq [Mf(1) + m(1)]\sqrt{GMR_0}, \tag{70}$$

where L_f is the total initial angular momentum left over at the end of the grain braking

era, M and $f(1)$ are the total mass and moment-of-inertia coefficient of the fully rotating cloud interior to the equatorial cylinder $s = R_e = R_0$ and $m(1)$ the mass of material exterior to that radius. Taking $L_f = 1 \times 10^{52} \mathrm{g\,cm^2 s^{-1}}$, from Equation (14), $f = 0.01$, $m(1)/Mf(1) = 0.3$ as typical values (see Section 6) we find that

$$R_0 \sim 16\,000\, R_\odot \tag{71}$$

i.e., the residual angular momentum left over at the end of the grain braking era is sufficient to cause the stabilized proto-stellar cloud first to become rotationally unstable at the periphery of the present planetary system. This meets a basic requirement for the validity of the Laplacian hypothesis.

5.2. Equations Governing the Exchange of Angular Momentum

As the proto-Sun collapses towards the radius R_0, conserving both total mass and total angular momentum, various changes take place as the rotational parameter Θ rises towards unity. Firstly, the originally nearly spherical convective envelope bulges outwards at the equator to assume a lenticular shape as described in Section 4. Secondly, the amount of material $m(\Theta)$ which can be supported outside the equatorial cylinder $s = R_e$ steadily increases to the maximum value $m(1)$ given by Equation (68). Expanding Equations (64), (65) to second order in the equatorial co-ordinates $\delta = s - R_e$, z and the parameter $1 - \Theta$, the density profile of the belt of non-turbulent equatorial gases is given by

$$\rho(\delta, z) = \rho_0 \exp\left\{-\alpha(\Theta)\left[(1-\Theta)\frac{\delta}{R_e} + \frac{1}{2}\frac{\delta^2}{R_e^2} + \frac{1}{2}\frac{z^2}{R_e^2}\right]\right\}. \tag{72}$$

From this equation it now follows, if we use Equations (58), (66), (68), that

$$\frac{m(\Theta)}{m(1)} = \left(\frac{2+\Theta}{3}\right)^4 \exp\left[\frac{\alpha(\Theta)}{2}(1-\Theta)^2\right]\left\{1 - \mathrm{erf}\left[\left(\frac{\alpha(\Theta)}{2}\right)^{1/2}(1-\Theta)\right]\right\}. \tag{73}$$

Since the mass of the equatorial belt of the fully rotating cloud exceeds that of the whole spherical shell of the non-rotating model by a factor of about 8, as mentioned at the end of Section 4.5, most of the material which goes into building the ring as the cloud contracts is new material which is freshly transferred across the photosurface from the convective interior. As the convective envelope extrudes this fresh material under conditions of uniform rotation, maintained throughout its interior by the supersonic turbulence, the angular velocity changes according to the equation

$$[M(\Theta)f(\Theta) + m(\Theta)]\,\omega_e R_e^2 = L_f, \tag{74}$$

whilst the total mass M_f of the system satisfies

$$M(\Theta) + m(\Theta) = M_f, \tag{75}$$

where $M(\Theta)$ is the mass interior to the equatorial cylinder $s = R_e$. In the case of a very

centrally condensed cloud, which is our regime of physical interest, we have (say)

$$f(\Theta) \ll 1, \quad m(\Theta) \ll M(\Theta) \simeq M(1) = M, \tag{76}$$

whilst $f(\Theta)$ changes according to Equation (59). In deriving Equation (74), the angular momentum of the equatorial ring of non-turbulent gases was computed using Equation (61). This equation corresponds to the conservation of local angular momentum for the non-turbulent gas which streams away from equatorial cylinder. The angular momentum per unit mass at the equator is $h_e = \omega_e R_e^2$. In fact, since h_e changes slightly as the proto-Sun is braked through the extrusion process, Equation (61) is only an approximation, as mentioned in Section 4.5, but as we shall show below in Section 5.4 only a very small error is induced through this simplification.

Lastly, since the equatorial radius R_e depends on the rotation parameter Θ through the definition

$$\Theta = \omega_e^2 R_e^3 / GM, \tag{77}$$

it is convenient to choose the polar radius R_p as the independent variable governing the size of the configuration since this evolves independently of the processes which take place at the equator. Now eliminating ω_e and R_e from Equation (74), we obtain by using Equations (58) and (70) the single equation

$$\Theta(R_p) = \left(\frac{R_{p_0}}{R_p}\right)\left(\frac{3}{2+\Theta}\right)\left\{\frac{1+\epsilon}{f(\Theta)/f(1) + \epsilon m(\Theta)/m(1)}\right\}^2 \tag{78}$$

where we define

$$\epsilon = m(1)/Mf(1), \tag{79}$$

and $R_{p_0} = \frac{2}{3}R_0$ is the polar radius when the proto-Sun becomes fully rotating at equatorial radius R_0. Substituting Equations (59) and (73), Equation (78) may be solved numerically to find Θ in terms of R_p for given values of ϵ and $\alpha(1)$.

5.3. NUMERICAL COMPUTATIONS

The results of the numerical computations for the typical cases $\epsilon = 2^{1/4} - 1$ and $\alpha(1) = 300, 1000$ are shown in Figure 6. There we find Θ and $m(\Theta)/m(1)$ plotted against the polar radius R_p in units of the value R_{p_0} at which $\Theta \to 1$. The dotted line in Figure 6 corresponds to the path which would be taken by a freely collapsing cloud which undergoes no structural changes as the degree of rotation increases. For such a collapse we have $\omega_e \propto 1/R_p^2$ and thus $\Theta = R_{p_0}/R_p$. The solution $\Theta = R_{p_0}/R_p$ is in fact the first-order iterative solution of Equation (78) obtained by setting $\Theta = 1$ throughout the right-hand side of this equation. We note that for large polar radii Θ precedes the value R_{p_0}/R_p corresponding to the 'rigidly' collapsing cloud but that as $R_p \to R_{p_0}$, Θ exceeds this value. This non-uniform behaviour is due to the changing equatorial structure of the proto-Sun. For $R_p \geqslant 1.5\, R_{p_0}$, Θ is small, $m(\Theta)/m(1)$ is small and the proto-Sun is nearly spherical (see Figure 5). During this interval it collapses nearly uniformly. Eventually as R_p becomes

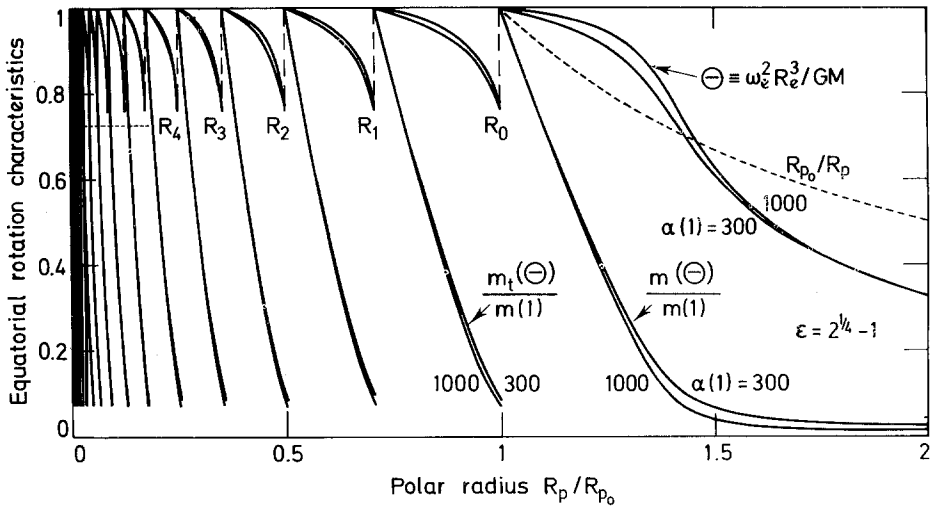

Fig. 6. Variation of the equatorial rotation parameter Θ_e as a function of polar radius R_p during the contraction. After each critical equatorial radius R_j ($j = 0, 1, 2, 3, \ldots$) has been passed, where $\Theta_e \to 1$, the proto-solar envelope rotationally stabilizes itself by extruding fresh material of mass $m_t(\Theta)$ to the equator. Two separate cases corresponding to the parameter $\alpha(1)$, given by Equation (66), are considered.

smaller, Θ increases faster than a $1/R_p$ law because of the growth in the equatorial radius R_e relative to R_p by the factor $(1 + \Theta/2)$. Beyond that stage when it approaches the limit $1.5\,R_p$ the rate of growth of Θ is rapidly curtailed as the bulk of the mass $m(\Theta)$ of the equatorial ring increases dramatically as $\Theta \to 1$, thereby rotationally braking the proto-Sun.

5.4. Mean Angular Momentum of the Equatorial Ring

Figure 7 shows a plot of the angular momentum per unit mass $h_e = \omega_e R_e^2$ at the equator of the proto-Sun in units of the value $h_0 = \omega_0 R_0^2 = \sqrt{GMR_0}$ at radius R_0, again for the cases $\epsilon = 2^{1/4} - 1$ and $\alpha(1) = 300$, 1000. We observe that initially $h_e < h_0$ when the cloud is nearly spherical. It then increases sharply as the equatorial region of the star becomes extended outwards by centrifugal force and lastly drops back to h_0 again at radius R_0 as the star becomes braked through the formation of the equatorial ring.

It is interesting to compute the mean orbital angular momentum per unit mass $\langle h_e \rangle$ of the material comprising the equatorial ring when the proto-Sun has contracted to the radius R_0. Throughout the analysis leading to Equation (78) we assumed that the angular velocity distribution in the ring is given by Equation (61) for which $\langle h_e \rangle = h_0$. In fact, since the mass $m(1)$ of the final ring is made up of material continuously extruded during the collapse we obtain for the case $\epsilon = 2^{1/4} - 1$

$$\langle h \rangle = \int_0^{m(1)} h(\Theta)\, \mathrm{d}m(\Theta)/m(1) \simeq \begin{cases} 1.01 h_0 \text{ if } \alpha(1) = 300, \\ 1.03 h_0 \text{ if } \alpha(1) = 1000. \end{cases} \tag{80}$$

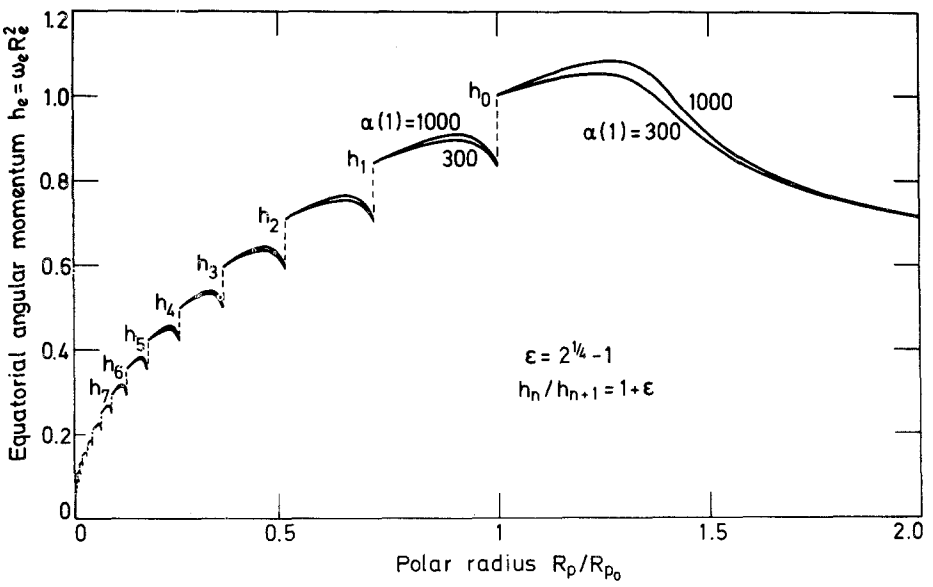

Fig. 7. Equatorial angular momentum per unit mass at various stages during the contraction. The sequence of values h_j at the critical points R_j in Figure 6, where $\Theta_e(R_j) = 1$, steadily decline as the shrinking envelope gives up its angular momentum through the extrusion and shedding of material at the equator.

This means that the final mean angular momentum per unit mass of the ring exceeds that at the equator of the fully rotating convective envelope by at most a few per cent. This means that as an improved approximation we should choose in place of Equation (61) a slightly less steep power law dependence for ω_e on s of the form

$$\omega_e(s, z) = \omega_e [R_e/s]^{2-\sigma}, \quad s \geqslant R_e. \tag{81}$$

To compute σ we insert Equation (81) in Equation (63) and integrate to obtain the density profile of the non-turbulent equatorial ring in the neighbourhood of the equator of the fully rotating cloud – viz.,

$$\rho(\delta, z) = \rho_e \exp\{-\tfrac{1}{2}\alpha(1)[(1-2\sigma)\delta^2 + z^2]/R_e^2\}. \tag{82}$$

Next, it follows that

$$\langle h \rangle = h_0/\sqrt{1-2\sigma}, \tag{83}$$

and, hence, comparing this with Equation (80) we see that

$$\sigma = 0.03 \ll 2. \tag{84}$$

Thus the approximation $\sigma = 0$ is in fact a very good one since to next order we should replace the term $(R_e/s)^2$ in Equation (61) by $(R_e/s)^{1.97}$ which is essentially the same. We therefore feel that the level of accuracy achieved through the initial assumption $\sigma = 0$ is sufficiently great to justify no further iteration for the solution $\Theta(R_p)$.

Lastly, we should mention that the physical significance of the angular velocity distribution given by Equation (81) is that the equipotential surfaces of the ring are distended outwards in the equatorial plane changing from being perfectly circular in meridional cross-section for $\sigma = 0$ to being slightly elliptic with semi-axes $1 + \sigma$, 1, respectively. In addition, since the mean angular momentum per unit mass exceeds the value at the equatorial radius R_0, where the angular velocity equals the Kepler velocity $\sqrt{Gm/R_0^3}$, if any gas should subsequently condense out as a solid and return to the radius R_0 it would inherit a positive (prograde) spin angular momentum equal to some 3% of the orbital angular momentum there.

6. Formation of the System of Gaseous Laplacian Rings

6.1. INTRODUCTION

Consider now the changes which take place near the equator of the proto-Sun after the fully rotating state has been attained at radius R_0. Because the proto-Sun is very strongly centrally condensed the central dense regions of the cloud barely feel the influence of rotation even when the centrifugal force at the equator balances the gravitational force. Consequently these regions will continue to contract inwards during the quasi-static collapse irrespective of the events which take place at the equator. If, however, the gravitational energy released throughout the cloud is sufficient to maintain a supersonic convective turbulence, then from thermodynamic considerations it follows that the run of density with temperature in the sub-photosurface regions of the cloud is preserved relative to those in the deep interior. Physically, however, no net outward transfer of heat from cloud can occur unless the temperature everywhere decreases outwards. If this condition is to be met it follows from the equation of hydrostatic support that we require

$$\Theta(R_e) \leqslant 1, \quad R_e \leqslant R_0, \tag{85}$$

as otherwise a temperature inversion would develop near the equator. Thus for a true convective equilibrium to exist it is necessary that the subphoto-regions of the cloud remain rotationally stable at all stages during the contraction.

In the next subsection we shall examine whether or not it is possible for the convective envelope to remain rotationally stable i.e. to satisfy Equation (85) during the contraction below polar radius R_{p_0}. Certainly it does not seem possible for the gases of the non-turbulent ring of material lying beyond the equatorial cylinder $s = R_e$ to remain rotationally stable once the cloud has contracted beyond the radius R_0, since if they should co-collapse with the cloud conserving their own angular momentum we should have at the equator

$$\Theta_{\text{ring}}(R_e) = R_0/R_e > 1, \quad \text{if} \quad R_e < R_0. \tag{86}$$

For the material of the convective envelope, interior to the equatorial cylinder, the

situation may not necessarily be the same since by transferring new material of mass m_t outwards from the deep interior of the cloud the envelope can be rotationally braked, the angular velocity being reduced by the factor $(R_0/R_e)^2/(1 + m_t/Mf)$. Thus, provided m_t is sufficiently great, we see that it may be actually possible for the proto-Sun to become rotationally stabilized again during the contraction below critical radius R_0, so that Equation (85) is always satisfied.

6.2. THE DISTRIBUTIONS OF PRESSURE AND DENSITY AND ANGULAR VELOCITY ABOVE THE PHOTOSURFACE

The sequence of events which accompany the collapse of the proto-Sun are illustrated in Figures 8 and 5. During the contraction of the convective envelope to a smaller equatorial radius R_e, a vacuum would be created in the space vacated by the equatorial cylinder $s = R_e$ if no material were to be transferred into that interval. If, however, the envelope is to maintain pressure equilibrium at its photosurface and the ring of non-turbulent gas lying beyond the cylinder $s = R_0$ is to maintain pressure equilibrium on the surface $s = R_0$ then material from both sides will pour inwards to fill the cylindrical annulus $R_e \leqslant s \leqslant R_0$. Thus as the convective envelope undergoes quasi-static collapse, new material from its deep interior will flow outwards across the equatorial cylinder $s = R_e$ and old material from the non-turbulent ring beyond radius R_0 will flow towards this radius until pressure equilibrium is established at each cylindrical radius. Let us denote by R_t the radius of the cylindrical surface of co-existence between the gases from the envelope and the ring. We may compute R_t as follows.

(i) *The Co-existence Cylinder* $s = R_t$

For the fresh non-turbulent material which flows outwards across the equatorial cylinder $s = R_e$, the angular velocity distribution is given by Equation (61), as justified in Section 5.4. Integrating the equation of hydrostatic support, viz Equation (63), the equilibrium density distribution becomes

$$\rho(s, z) = \rho_e(R_p) \exp\left\{\alpha(\Theta)\left[\frac{R_e}{r} - 1 + \frac{\Theta}{2}(1 - R_e^2/s^2)\right]\right\}, \qquad R_e \leqslant s \leqslant R_t. \tag{87}$$

where $\rho_e(R_p)$ is the density of non-turbulent gas at the equator. As long as the collapse of the polar regions of the proto-Sun occur homologously then

$$\rho_e(R_p) = \rho_e(R_{p_0})(R_{p_0}/R_p)^3, \tag{88}$$

and, similarly, for the temperature distribution above the photosurface we have assumed that

$$T(s, z) \overset{\Psi \leqslant 0}{=} T_e(R_p) = T_e(R_{p_0})(R_{p_0}/R_p), \tag{89}$$

whilst $\alpha(\Theta)$ is given, as before, by Equation (66).

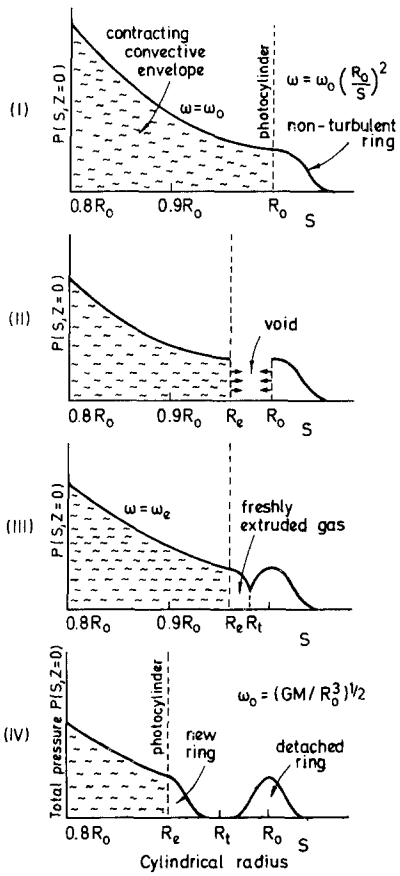

Fig. 8. Distribution of total pressure p with cylindrical polar radius s in the vicinity of the equator in the equatorial plane at various stages of the contraction of the envelope through the first critical point $R_e = R_0$. In order to maintain pressure equilibrium at the photosurface, the convective envelope extrudes fresh material into the cylindrical void $R_e < s < R_t$, where the co-existence cylinder $s = R_t$ is given by Equation (92). In extruding this fresh material of mass m_t from the deep interior of the cloud under conditions of uniform rotation, maintained by the supersonic turbulent convection, the envelope is rotationally stabilized provided m_t is sufficiently large, that is (see Equation (113) and Figure 9), if the turbulence is sufficiently strong.

Consider next the material of the gaseous ring lying beyond the cylinder $s = R_0$. As the proto-Sun contracts, this material expands freely into the interval $R_t \leqslant s \leqslant R_0$ conserving its angular momentum. The angular velocity distribution of this material is, therefore, given by

$$\omega(s, z) = (GM/R_0^3)^{1/2}(R_0/s)^2 . \tag{90}$$

For the sake of simplicity we assume a constant temperature distribution throughout the non-turbulent material, the same as Equation (89). In fact, as we shall later point out, the black-body temperature in the gas declines according to the law $T \simeq T_e(R_e/s)^{1/2}$ as one moves away from the proto-Sun in the equatorial plane. But as the effective thickness

of the ring turns out to be very much smaller than the radius R_0, this modification in the temperature profile produces a variation which is negligible in comparison to the other changes going on at the equator, and so will be ignored.

Now integrating the equation of hydrostatic support we obtain for the density profile beyond the cylinder $s = R_t$

$$\rho_r(s, z) \underset{s \geqslant R_t}{=} \rho_0(R_0) \exp\left\{\alpha(\Theta)\frac{R_e}{R_0}\left[\frac{R_0}{r} - \frac{1}{2}\frac{R_0^2}{s^2} - \frac{1}{2}\right]\right\}, \tag{91}$$

where $\rho_0(R_0)$ is the density on the circular axis $s = R_0$, $z = 0$. On this axis the angular velocity equals the local Kepler value $(GM/R_0^3)^{1/2}$ and the density is a maximum, as shown in Figure 8. Initially $\rho_0(R_0) = \rho_e(R_{p_0})$ but as the proto-Sun recedes and the old gaseous ring left behind at radius R_0 distributes itself uniformly about the Keplerian axis $s = R_0$, we have $\rho_0(R_0) \to \frac{1}{2}\rho_e(R_{p_0})$, its total mass remaining constant as given by Equation (68).

Now equating $\rho(s, z)$ and $\rho_r(s, z)$ and noting that for $\alpha(\Theta) \gg 1$ it is sufficient to equate the exponents of equations (87), (91) we find that the radius of the co-existence cylinder is

$$R_t = R_0\left[\frac{R_e}{R_0}\frac{1 - \Theta R_e/R_0}{2 - \Theta - R_e/R_0}\right]^{1/2}. \tag{92}$$

At this radius the outward pressure of the fresh material extruded from the convective envelope balances the inward radial stress of the material of the gaseous ring centred on radius R_0. For Θ close to 1 we see that R_t lies approximately mid-way between R_e and R_0. The density at the interface is thus approximately

$$\rho_t \simeq \rho_0(R_0) \exp\left[-\tfrac{1}{8}\alpha(\Theta)(R_0/R_e - 1)^2\right]. \tag{93}$$

Since this is negligible in comparison with the central ring density $\rho_0(R_0)$ for

$$|R_e - R_0| \gtrsim 2R_0\left[2/\alpha(\Theta)\right]^{1/2} \sim 0.1\,R_0, \tag{94}$$

we see that the gaseous ring essentially detaches itself from the proto-Sun once the equatorial radius of the latter has shrunk to about $0.9\,R_0$.

It is worth noting that although the total gas pressure $p = \rho\mathscr{R}T/\mu$ is continuous across the co-existence cylinder $s = R_t$, the angular velocity distribution is not so. At the interface, the angular speed of the material just interior to this point is $[\Theta GM/R_e^3]^{1/2}(R_e/R_t)^2 < (GM/R_t^3)^{1/2}$ if $\Theta < 1$, whilst just exterior to this radius it is $(GM/R_0^3)^{1/2}(R_0/R_t)^2 > (GM/R_t^3)^{1/2}$. The two species of gas on either side of the cylinder may, therefore, tend to mix together, thus altering the distribution of angular velocity and density at this point. Nonetheless, if Equation (94) is satisfied so that ρ_t is negligible, then we do not expect mixing to be important, especially if the rate of collapse of the proto-Sun is fast compared to the viscous time scale of the small-scale fluid turbulence which is generated by the discontinuity of angular velocity. We shall return to this point in Paper II.

6.3. ROTATIONAL EVOLUTION OF THE PROTO-SUN

We are now in a position to write down the equations which govern the rotational evolution of the proto-Sun as the polar radius shrinks below the critical value R_{p_0}. Using the same approximations as described in Section 5 under Equation (76) the equation for conservation of total angular momentum of material interior to the cylinder $s = R_t$ is of the form

$$[Mf(\Theta) + m_t(\Theta)]\,\omega_e R_e^2 = L_0 \equiv Mf(1)\sqrt{GMR_0}, \tag{95}$$

where L_0 is the initial angular momentum interior to the equatorial cylinder $s = R_0$ and m_t the mass of freshly extruded gas when the protosun has shrunk to polar radius R_p. Expanding Equation (87) to second order in the local equatorial co-ordinates $\delta = s - R_e$, z we obtain

$$\begin{aligned} m_t(\Theta) = m(1)\left(\frac{2+\Theta}{3}\right)^4 \exp\left[\frac{\alpha(\Theta)}{2}(1-\Theta)^2\right] \\ \times\left\{\operatorname{erf}\left[\left(\frac{\alpha(\Theta)}{2}\right)^{1/2}\left(\frac{R_t}{R_e}-\Theta\right)\right] - \operatorname{erf}\left[\left(\frac{\alpha(\Theta)}{2}\right)^{1/2}(1-\Theta)\right]\right\}, \end{aligned} \tag{96}$$

where $m(1)$, as in Equation (73), is the total mass of the old gaseous ring, detached at radius R_0. Eliminating ω_e, R_e with Equations (58), (77), (95) we arrive at the single equation

$$\Theta(R_p) = \left(\frac{R_{p_0}}{R_p}\right)\left(\frac{3}{2+\Theta}\right) \Big/ \left\{\frac{f(\Theta)}{f(1)} + \epsilon m_t(\theta)/m(1)\right\}^2, \tag{97}$$

where ϵ is defined by Equation (79).

(i) *Numerical Computations*

The numerical solution of Equations (96), (97) for $\Theta(R_p)$ and m_t are shown in Figure 6 to the left of the ordinate line R_{p_0} again for the typical cases $\epsilon = 2^{1/4} - 1, \alpha(1) = 300$, 1000. The dashed line shows m_t in units of $m(1)$.

Several interesting features of the solutions are worth discussing. Firstly we observe that Θ and hence the other physical characteristics R_e and $f(\Theta)$ of the protosun behave discontinuously immediately the structure contracts inwards from the fully rotating configuration at polar radius R_{p_0}. Since the equatorial radius of the convective envelope is given by $R_e = R_p(1 + \Theta/2)$ it follows from Figure 6 that there exist no equilibrium configurations having radius R_e between about $0.9R_0$ and R_0. Instead, as the polar radius shrinks by an infinitesimal fraction below R_{p_0}, the equatorial radius appears to withdraw discontinuously onto a new solution branch corresponding to a state of rotational stability. The physical reason for this discontinuous behaviour resides in the critical structure of the fully rotating convective envelope. The angular momentum L_0 of this envelope is reduced by a small amount $\Delta L = L_0\delta/f(1)$ whenever a correspondingly small small amount of mass

$$\Delta m = \delta M, \quad \delta \ll 1, \tag{98}$$

is transferred outwards to the equator. Such a change induces a very much larger change $\Delta\Theta = -\sqrt{6\delta/f(1)}$ in Θ using Equations (59), (79), (97) and hence a change

$$\Delta R_e = -(\tfrac{2}{3}\delta/f(1))^{1/2} R_0 \tag{99}$$

in the equatorial radius. Next it follows from Equations (92), (96) that for pressure equilibrium to be established at the photosurface Δm must satisfy the additional relation

$$\Delta m \propto (R_t - R_e) R_0^2 \rho_e(R_{p_0}) \propto \delta^{1/2} M. \tag{100}$$

Comparing Equations (98), (99) we see that analytically it is not possible to construct a consistent continuous solution for Θ in the neighbourhood of R_{p_0} with the property $\Theta \to 1$ as $R_p \to R_{p_0}$ from below; that is, Θ moves discontinuously to a new solution branch as soon as the proto-Sun contracts past the critically rotating radius.

(ii) *Detachment of the Gaseous Laplacian Ring*

As the equatorial regions of the convective envelope withdraw catastrophically* from the radius R_0, the ring of gaseous material lying beyond the cylinder $s = R_0$ rushes in after them distributing itself symmetrically about the Keplerian axis $s = R_0$, $z = 0$ with angular velocity distribution given by Equation (90) and density distribution given from Equation (91) by

$$\rho_r(\delta, z) \simeq \rho_0(R_0) \exp\left[-\tfrac{1}{2}\alpha(\Theta)\xi^2 R_e/R_0^3\right], \tag{101}$$

where $\xi^2 = (s - R_0)^2 + z^2$. When the envelope reattains a consistent pressure equilibrium at its photosurface at radius $R_e \sim 0.9 R_0$ it follows from Equation (94) that the density at the interface R_t is $\rho_t \ll \rho_0(R_0)$. Therefore the proto-Sun literally detaches itself from non-turbulent material lying beyond the equatorial cylinder as soon as the radius R_0 is reached. This material is left behind at radius R_0 as an isolated secondary structure supported through a balance between centrifugal force and the gravitational field of the proto-Sun. This ring of gas abandoned by the collapsing proto-Sun in its equatorial plane may be called a Laplacian ring.

(iii) *A Return to the State of Rotational Instability at Radius* R_1

The second main feature which we observe in Figure 6 is that the rotation parameter rises to unity again when the proto-Sun shrinks to the new critical radius $R_1 = R_0/\sqrt{2}$. This behaviour follows from Equations (96), (97). The proto-Sun is initially strongly rotationally stabilized through the transfer of new material of mass m_t to the equator, causing the angular velocity to decline according to the law

$$\omega_e = \omega_0 \left(\frac{R_0}{R_e}\right)^2 f(1)/[f(\Theta) + m_t(\Theta)/M]. \tag{102}$$

* That is, dynamically, on a free-fall time-scale, rather than quasi-statically as prior to radius R_0.

Eventually as R_e gets smaller the reduction in ω_e achieved by the factor $f(1)/[f(\Theta) + m_t(\Theta)/M]$ is overtaken by the growth of the factor $(R_0/R_e)^2$ until a radius R_1 is reached, given by

$$R_0/R_1 = [1 + m(1)/Mf(1)]^2 = (1 + \epsilon)^2, \tag{103}$$

where

$$\omega_e^2(R_1) = GM/R_1^3, \quad \Theta(R_1) = 1, \tag{104}$$

and

$$m_t(1) \simeq m(1), \tag{105}$$

provided that

$$\left(\frac{\alpha(1)}{2}\right)^{1/2} \left[\sqrt{\frac{R_0}{R_1}} - 1\right] = \epsilon\left(\frac{\alpha(1)}{2}\right)^{1/2} \gtrsim 1. \tag{106}$$

Although ϵ depends on the turbulence parameter β, polytropic index n and photosurface temperature ratio θ_{ph} and has yet to be computed, it is a simple matter to show that the inequality in Equation (106) is easily satisfied for the case $\epsilon = 2^{1/4} - 1$. For this value of ϵ we have $R_0/R_1 = \sqrt{2}$.

Thus, as R_e shrinks to R_1, the convective envelope finds itself returning to the critical state again whilst the cylindrical shell of newly extruded material in the interval $R_e \leqslant s \leqslant R_t$ assumes a ring-like structure which is essentially identical to the ring of material which previously existed beyond the cylinder $s = R_0$, except that its density profile terminates at the co-existence cylinder $s = R_t$, where

$$R_t = \sqrt{R_0 R_1} = R_1(1 + \epsilon). \tag{107}$$

(iv) *A Repeated Process*

Once the envelope becomes fully rotating again at radius R_1 and continues to contract inwards the whole process of ring detachment followed by growth of a new ring repeats itself and again at the sequence of critical points R_2, R_3, R_4 etc as shown in Figure 6. That is, the turbulent convective proto-Sun disposes of its excess angular momentum through the formation of a system of gaseous Laplacian rings.

6.4. THE TITIUS-BODE LAW

As long as the collapse of the polar regions of the envelope take place nearly homologously so that $f(1)$ and $m(1)/M$ remain constant, then the ratio of the orbital radii R_j of the successively disposed gaseous Laplacian gaseous rings is simply

$$\frac{R_j}{R_{j+1}} = \left(1 + \frac{m(1)}{Mf(1)}\right)^2 = \text{constant}, \tag{108}$$

with $j = 0, 1, 2, 3, 4 \ldots$; that is, the set of orbital radii R_j form a geometric sequence

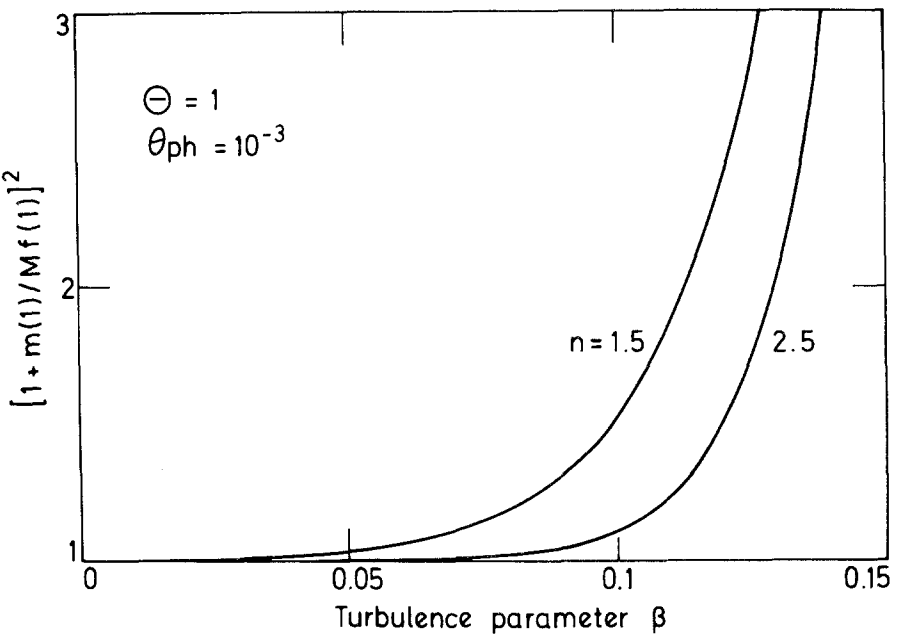

Fig. 9. Plot of ring-spacing factor $R_j/R_{j+1} = \{1 + m(1)/Mf(1)\}^2$ as a function of the turbulence parameter β. Unless $\beta \geqslant 0.05$ the rings become so closely spaced that the analysis leading to Equation (103) ceases to be valid and the star is unable to rotationally stabilize itself through equatorial mass shedding, even if it shed material continuously.

which is similar to the Titius-Bode law for the distribution of planetary distances and those of the satellite systems of the major planets. According to our theory the value of the Titius-Bode constant depends on both the degree of turbulence β as well as $\theta_{\rm ph}$ and the polytropic index n and is given by

$$\Gamma \equiv \langle R_i/R_{i+1}\rangle = (1+\epsilon)^2, \quad \epsilon = \pi\left(\frac{3}{2}\right)^7 (\beta + 1/\alpha(0))\,\frac{\rho_c \theta_{\rm ph}^n}{\bar{\rho} f(0)}, \tag{109}$$

where, using the notation of Section 4, $\rho_c/\bar{\rho}$ and $f(0)$ are the ratio of central to mean density and moment-of-inertia coefficient of the non-rotating structure of the same polar radius as that of the fully rotating proto-Sun.

We have plotted Γ vs. β in Figure 9 for the typical cases $\theta_{\rm ph} = 10^{-3}$ and $n = 1.5$, 2.5. We observe with interest that in order to account for the observed spacing of the planetary distances, where $\Gamma_{\rm obs} = 1.73$, $\epsilon_{\rm obs} \simeq 0.3$, we require a turbulence parameter β of order 0.1. This value is a typical one for the theory of supersonic convective turbulence which we have so far developed.

(i) *A Necessary Condition for the Shedding of a System of Laplacian Rings*

It is also interesting to note from Figure 9 that as the degree of turbulence declines, the spacing between the rings becomes smaller and in fact becomes essentially zero

($\sim 10^{-3}$) in the non-turbulent limit $\beta = 0$. In fact it is not possible for a weakly turbulent protosun to rid itself of its excess angular momentum in the manner we have proposed unless the condition specified in Equation (106) is satisfied. To appreciate this point we consider the first-order continuous solutions for m_t and Θ in the neighbourhood of the radius R_0 obtained by setting $\Theta = 1$ throughout the right hand side of Equations (92), (96), (97). We obtain

$$m_t^{(i)}(R_e)/m(1) = \operatorname{erf}\left[\left(\frac{\alpha(1)}{2}\right)^{1/2}\left(\sqrt{\frac{R_0}{R_e}}-1\right)\right] = \left(\frac{\alpha(1)}{2\pi}\right)^{1/2}(R_0 - R_e) + \ldots, \tag{110}$$

$$\Theta^{(i)}(R_e) = 1 - [\epsilon(2\alpha(1)/\pi)^{1/2} - 1](R_0 - R_e) + \ldots \tag{111}$$

Inspecting Equation (111) we see that the proto-Sun is rotationally stabilized through the outward extrusion of material to the equator only if

$$\epsilon(2\alpha(1)/\pi)^{1/2} \geqslant 1; \tag{112}$$

or, equivalently, if we use Equation (109), if

$$\beta \geqslant \frac{(2/3)^{13/2}}{\sqrt{2\pi\alpha(0)}}\frac{\bar{\rho}}{\rho_c}\frac{f(0)}{\theta_{\mathrm{ph}}^n} \sim 0.05 \tag{113}$$

for the typical case $n = 1.5$, $\theta_{\mathrm{ph}} = 10^{-3}$. Equation (112) is essentially identical to the earlier derived Equation (106).

Equation (113) tells us that unless the turbulence is sufficiently strong, the amount of angular momentum shed at the equator through the formation of a system of Laplacian rings is insufficient to keep the convective envelope rotationally stable during the contraction. The mass of the equatorial rings depends on the ratio of turbulent stress to gas pressure ratio at the photosurface, as we note from Equations (47) and (68). For the weakly turbulent star, $m(1)$ is too small to allow the convective envelope to safely contract. The outer layers of a weakly turbulent cloud therefore probably become successively stripped away during its collapse as the point where $\Theta = 1$ steadily works its way towards the centre of the object. This phenomenon has been studied both by Hoyle (1960) and Cameron (1962). The physical but unobserved outcome of such a collapse is a vast disc-like nebula possessing no central condensation, or the Sun.

We conclude that supersonic turbulent convection is not only essential to the efficient disposal of angular momentum through the process of equatorial mass shedding, but is also crucial to our understanding of why the proto-Sun shed its excess angular momentum through the formation of a discrete system of Laplacian rings.

6.5. THE PROGRESSIONS OF RESIDUAL MASS AND ANGULAR MOMENTUM

The residual angular momentum of the proto-Sun after the disposal of the jth gaseous ring at orbital radius R_j scales according to the geometric progression

$$L_j = L_0 \Big/ \left[1 + \frac{m(1)}{Mf(1)}\right]^j = L_0 \left(\frac{R_j}{R_0}\right)^{1/2}, \tag{114}$$

where L_0 is given by Equation (95). Thus we see that during its collapse from radius about $10^4 R_\odot$ to $R_\odot$, the proto-Sun is able to lose two orders of magnitude of angular momentum through the process of shedding rings of gas at its equator. At the same time the mass M_j left over after the disposal of the jth ring scales as

$$M_j = M_0 \left(1 - \frac{m(1)}{M_0}\right)^j \simeq M_0 \left(\frac{R_j}{R_0}\right)^{f(1)/2}. \tag{115}$$

Again with $R_j/R_0 = 10^{-4}$, $f(1) = 0.01$ we find the proto-Sun only loses about 5% of its original mass during the entire collapse. That is, the mass hardly changes during the contraction compared to the loss in angular momentum. The physical reason for this event lies, of course, in the immense degree of central condensation, or very low moment-of-inertia coefficient, achieved through the supersonic turbulent convection.

According to our theory the proto-Sun arrives at stellar size still spinning very rapidly with a period of the order of a few hours. In fact, as we shall point out in the next section, the rate of collapse of the proto-Sun drastically declines during the final stages from a radius of about $30 R_\odot$ down. This may allow time for other angular momentum braking processes, such as the interaction of a solar wind with any small-scale magnetic fields generated by small-scale turbulence below the photosurface to rid the proto-Sun of its last vestige of angular momentum.

6.6. A COMPUTATIONAL SUMMARY

The equations which govern the distribution of density and angular velocity in the concentric system of gaseous rings abandoned by the contracting proto-Sun at the sequence of orbital radii $R_0, R_1, \ldots, R_n$ are as follows. For the nth gaseous ring of mass $m(1)$ and assumed constant temperature T_n we have

$$\rho_n(s, z) = \rho_0(R_n) \exp(\alpha_n \Psi_n) \tag{116}$$

$$\omega_n(s, z) = \sqrt{GMR_n}/s^2, \tag{117}$$

where

$$\rho_0(R_n) \simeq \alpha_n m(1)/4\pi R_n^3 \tag{118}$$

is the density on the circular Keplerian orbit $s = R_n$, and

$$\alpha_n = \mu GM/\mathscr{R} T_n R_n, \tag{119}$$

$$\Psi_n = \left[\frac{R_n}{r} - \frac{1}{2}\left(\frac{R_n}{s}\right)^2 - \frac{1}{2}\right] \simeq -[(s - R_n)^2 + z^2]/2R_n^2. \tag{120}$$

The location of the surfaces separating the nth and $(n+1)$th rings follows from the equation $\rho_n(s, z) = \rho_{n+1}(s, z)$ and depends on the choice of the temperature distribution T_n. We assume a black body distribution

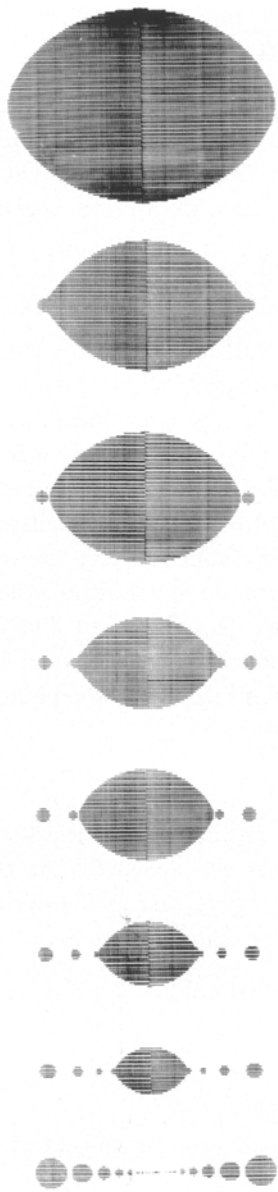

Fig. 10. Meridional cross-section of the contracting proto-Sun and its system of gaseous rings at various stages during the contraction. The shaded regions correspond to all mass points interior to the equipotential surfaces $\alpha(1)\Psi = \alpha_n\Psi_n = -2$, given by Equations (64), (65), (119), (120) and (123), taking $\overset{*}{\alpha}(1) = 1000$. Thus in the vicinity of each gaseous ring at radius R_n the shaded region corresponds to the points for which $\rho > \rho_0(R_n)\exp(-2)$ where $\rho_0(R_n)$ is the density on the circular axis of the ring, which decreases outwards with R_n in accord with Equation (118).

(121) $$T_n \simeq T_e[R_e/R_n]^{1/2}, \tag{121}$$

corresponding to a nearly transparent nebula surrounding a proto-Sun of temperature T_e and equatorial radius R_e. In that case, the surface where the nth and $(n+1)$th gaseous rings merge is nearly coincident with a cylinder of radius R_{t_n} given by

$$R_{t_n} = \sqrt{R_n R_{n+1}} \left\{ \left(\frac{R_n}{R_{n+1}} \right)^{1/4} + \left(\frac{R_{n+1}}{R_n} \right)^{1/4} - 1 \right\} \simeq \sqrt{R_n R_{n+1}}. \tag{122}$$

In Figure 10 we have computed the meridional, or polar, cross-section of the proto-Sun and its attendant system of disposed gaseous rings at various stages of the gravitational contraction. The shaded zones correspond to regions where for each ring the density exceeds $e^{-2}\rho_0(R_n)$, where $\rho_0(R_n)$ is the density on the mean orbit $s = R_n$, on which it is a local maximum, and for the protosun where the density exceeds $e^{-2}\rho_e(R_e)$, where $\rho_e(R_e)$ is the density at the equator as in Equations (64), (65) and (87). Mathematically, therefore, the shaded areas correspond to the interior of the equipotential surfaces $\alpha(1)\Psi(s, z) = -2$, $\alpha_n \Psi_n(s, z) = -2$, $n = 0, 1, 2, 3, \ldots$, since from Equations (58), (66) and (119) we note that

$$\alpha_n = \alpha(1) \left(\frac{3}{2 + \Theta} \right) \sqrt{R_e/R_n}, \tag{123}$$

where Θ is the rotation parameter of the proto-Sun which varies during the collapse in accord with Figure 6. For the purposes of the calculation we have chosen the case $\alpha(1) = 1000$.

We observe in Figure 10 that the outer gaseous rings command a greater volume than the inner ones. This is a characteristic feature of the homologous nature of the contraction. For rings of constant mass $m(1)$ the density scales outwards with R_n according to Equation (119) owing to the fact that the ratio of the volume of a detached ring to that of the proto-Sun at the moment of detachment is preserved during the contraction. The inner gaseous rings are, therefore, much denser than the outer ones. The effective minor radius ξ_n of each ring shown in Figure 10 is given from Equations (116) and (121) by

$$\xi_n = 2R_n/\sqrt{\alpha_n} \simeq \frac{2R_n}{\sqrt{\alpha(1)}} (R_n/R_e)^{1/4}, \tag{124}$$

noting that the proto-solar temperature T_e varies during homologous contraction as R_e^{-1}. Initially, at the moment of detachment, when $R_e = R_n$ we have $\xi_n \simeq 0.06 R_n$, taking $\alpha(1) = 1000$. Thereafter as the proto-Sun grows hotter during the contraction and the temperature T_n at each fixed point R_n increases as $T_n \propto R_e^{-1/2}$, the rings of gas warm up and undergo thermal expansion. This effect is more pronounced in the outermost rings, as we note in the diagram. Typically, taking $R_e = 50 R_\odot$, $R_n = 5000 R_\odot$ we find $\xi_n/R_n = 0.20$. Since the observed mean orbital distance between adjacent rings $R_n - R_{n+1} = 0.73 R_{n+1}$ always exceeds the sum of the minor radii $\xi_n + \xi_{n+1}$, we see that system of rings maintains its discrete structure during the proto-Sun's contraction. Ultimately, for

$R_e \lesssim 20 R_\odot$, the homologous character of the collapse disappears and the rings commence to shrink in thickness again as the proto-Sun moves towards the Main Sequence and the temperature throughout the solar system declines, as we shall discuss in more detail in the next section.

The above analysis, of course, supposes that each ring maintains the angular velocity distribution given by Equation (117). In fact, as we shall discuss in Paper II, it is possible that the dense inner rings of the solar nebula may become thermally convective when the proto-Sun enters its most luminous phase at radius $R_e \simeq 20 R_\odot$, causing ω_n to be rendered uniform and the rings to physically disintegrate. In any event, we feel that Figure 10 shows how during the contraction through the dimensions of the planetary system, the protosun sheds a well-defined system of circularly orbiting gaseous Laplacian rings, lying in its equatorial plane.

7. Influence of Internal Thermodynamic Changes on the Physical Characteristics and Rate of Collapse of the Proto-Sun

7.1. INTRODUCTION

In Section 5.4 we discovered that if the contraction of the proto-Sun occurs homologously during the interval from $10^4 R_\odot$ to $10^2 R_\odot$ then the orbital radii of the successively disposed gaseous rings satisfy a geometric relationship similar to the Titius-Bode law. Now although it seems physically reasonable that the contraction should take place uniformly if the various physical parameters β, $\theta_{\rm ph}, \ldots$ of the cloud remain constant, this conclusion is far from obvious when one considers the various thermodynamic changes (dissociation of H_2, ionization of H, He) which inevitably take place during the course of the collapse and which drastically alter the internal distribution of temperature and density inside the cloud. In this section therefore we shall investigate the influence of these atomic and molecular changes on the homologous nature of the contraction. We also consider the final stages of the pre-Main-Sequence collapse for radii $R_e \lesssim 20 R_\odot$ where photospheric conditions force us to abandon the constraints that $\theta_{\rm ph}$ as well as perhaps β remain constant. The detailed calculations of Ezer and Cameron (1965) and Hoyle and Wickramasinghe (1968) suggest that the surface temperature of the proto-Sun in the final stages of contraction levels off to about 4500 K rather than continuing to increase according to the law $T_e \propto R_e^{-1}$ as in a homologous contraction.

7.2. COMPUTATIONAL PROCEDURE

Proceeding as in Section 3.2 we suppose that for any given equatorial radius R_e the proto-Sun may be divided into an inner region of fractional mass q_1 and polytropic index $n_1 = 3/2$, in which the H is all fully dissociated, surrounded by an outer region in which the H is fully molecular, for which the polytropic index is given by Equation (36). For any given q_1, β, $\theta_{\rm ph}$ the equatorial radius R_e of the configuration is uniquely determined from the condition that the concentrations of H and H_2 are equal at the

interface q_1. Initially we suppose that β, θ_{ph} are constant so that departures from uniform contraction occur solely through the variations of q_1. As the cloud becomes smaller, however, and heats up, q_1 steadily increases and approaches unity at a radius $R_{e,*} \sim 20 R_\odot$ where the surface temperature is $T_* \sim 3500$ K. Beyond this point it is not possible to suppose that θ_{ph} remains constant during the subsequent contraction to radius $R_e = 1.5 R_\odot$ (for a fully rotating sun $R_e = 1.5 R_p$) since this would lead to a final photosurface temperature of order $\sim 10^5$ K. Instead as soon as $q_1 \to 1$ we adopt a photosurface temperature law of the form

$$T_{ph}(R_e) \; {}^{R_e \leqq R_{e*}} \; 4500(T_*/4500)^y \text{ K}, y = \left| \frac{\log (R_e/1.5 R_\odot)}{\log (R_{e,*}/1.5 R_\odot)} \right|^2, \quad (125)$$

which matches on to the more detailed calculations of Ezer and Cameron (1965) as $R_e \to 1.5 R_\odot$. In addition, since the levelling off of $T_{ph}(R_e)$ drastically lengthens the time-scale

$$\tau_{KH} \simeq C_n G M^2 / R_e^3 T_{ph}^4 \quad (126)$$

for the disposal of the excess gravitational energy as R_e gets smaller, it is reasonable to suppose that the supersonic turbulence starts to die down in this final stage of the contraction. To present this feature explicitly we suppose that β declines in a manner such that the proto-Sun moves on to the zero-age Main Sequence preserving its central density profile so that the moment-of-inertia coefficient remains constant: namely,

$$f = f_* \equiv f(R_{e,*}) \simeq 0.02. \quad (127)$$

For a non-rotating proto-Sun this implies a final f of ~ 0.05 which is closely representative of the value expected for the Sun (Allen, 1962).

7.3. Influence of the Dissociation of H_2 on the Physical Characteristics of the Proto-Sun

Figures 11 and 12 show the influence of the dissociated core mass fraction q_1 on various physical characteristics of the fully rotating ($\Theta_e = 1$) cloud for the case $\theta_{ph} = 10^{-3}$ and $X = 0.7$, $Y = 0.3$. The quantities plotted are the ratio of central to mean density $\rho_c/\bar{\rho}$, the ratio P_{ph} of turbulent stress to gas pressure at the photosurface, the gravitational potential energy concentration factor $C_n(\beta, 1)$ defined by Equations (23), (31) and the central temperature T_c expressed in units of $\mu_c GM/\mathscr{R}R_e = 2.291\ \mu_c(R_\odot/R_e) \times 10^7$ K, where μ_c is the central molecular weight. Figure 12 shows the mass $m(1)$ of the equatorial gaseous ring in units of the mass M of the turbulent envelope, the moment-of-inertia coefficient $f(1)$ of the envelope and the Titius-Bode function $[1 + m(1)/Mf(1)]^2$.

We observe from the behaviour of $\rho_c/\bar{\rho}$, C_n and T_c as functions of q_1 that as the dissociated core mass spreads outwards the cloud becomes less centrally condensed. This is due to the lowering of the effective polytropic index $\bar{n}$ of the cloud which passes from 2.324 for $q_1 = 0$ to 1.5 for $q_1 = 1$. The greater the fraction of H_2 the larger the mean number of degrees of freedom $\bar{\nu}$ and hence the larger $\bar{n} = \bar{\nu}/2$.

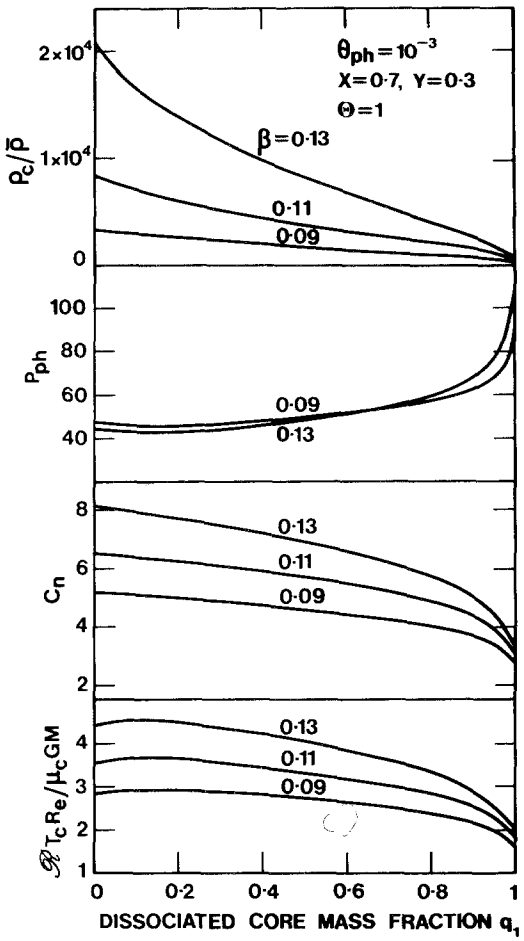

Fig. 11. Physical characteristics of fully rotating turbulent polytropic protosolar models consisting of an inner dissociated core mass of mass fraction q_1 and polytropic index $n = 1.5$ surrounded by an outer layer of index n given by Equation (36) in which the H is mostly molecular.

Consider next Figure 12. We note with interest that the mass $m(1)$ of the equatorial ring and the Titius-Bode function $[1 + m(1)/Mf(1)]^2$ remain practically constant over almost the entire range of the parameter q_1. This means that despite the vast changes which take place in the thermodynamic state of the cloud during its contraction, the masses of the disposed gaseous rings are all much the same and their orbital radii R_n satisfy a roughly geometric relationship. That is, a Titius-Bode law still emerges even when the variations induced by the dissociation of H_2 are included, which is certainly a remarkable result. Physically this result follows from the fact that the mass $m(1) = 2\pi^2 R_e^4 P_{tot}(R_e)/GM$ and $f(1)$ depend only on the total pressure $P_{tot}(R_e)$ at the equator and the internal run of density with radius. Since for a strongly turbulent star the gas pressure $\rho\mathscr{R}T/\mu$ is negligible compared to the turbulent stress $\beta\rho GM(r)/r$ over almost all

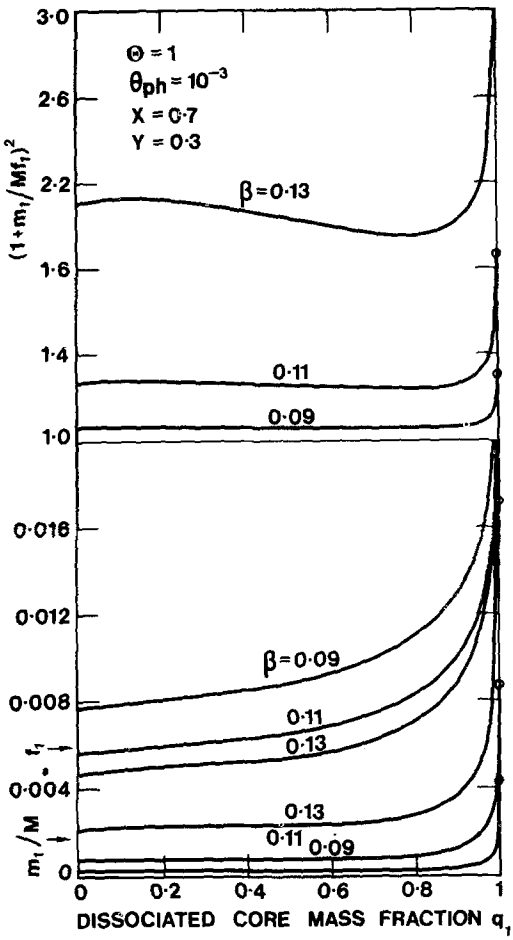

Fig. 12. Equatorial ring mass $m(1)$, envelope moment-of-inertia coefficient $f(1)$, and ring-spacing variable $\{1 + m(1)/Mf(1)\}^2$ of two-layered turbulent polytropic structures, as in Figure 11.

of the radius r, so that $P_{\rm tot} \simeq \beta\rho GM(r)/r$ it follows from the hydrostatic support equation, namely $\nabla P_{\rm tot} = -\rho GM(r)\mathbf{r}/r^3$ ignoring rotation, that the behaviour of $\rho(r)$ and $P_{\rm tot}(r)$ is largely independent of the behaviour of polytropic index n and temperature T/μ, and hence of the location of q_1. That is, $m(1)$ and $f(1)$ are approximately independent of q_1.

The variation of the physical characteristics with respect to changes in β are in accord with our descriptions given earlier in Sections 3 and 4. To produce a planetary (or satellite) system with a Titius-Bode constant $\langle R_n/R_{n+1}\rangle = 1.3 - 2.1$ we see we typically require the turbulence parameter β to lie in the range 0.11 to 0.13, selecting $\theta_{\rm ph} = 10^{-3}$. Otherwise setting $\beta = 0.12$ we require a variation of photospheric temperature ratio $\theta_{\rm ph}$ in the interval $0.0005 \leqslant \theta_{\rm ph} \leqslant 0.002$.

7.4. VARIATIONS WITH RESPECT TO THE EQUATORIAL RADIUS R_e; THE TITIUS-BODE FUNCTION

Consider now Figures 13, 14 and 15 which show the variation of the Titius-Bode variable $[1 + m(1)/Mf(1)]^2$ and surface temperature T_e with equatorial radius R_e and the variation of R_e with time elapsed during the contraction from radius $10^4 R_\odot$. We see from Figure 13 that during the collapse through the dimensions of the present planetary system, from about $10^4 R_\odot$ to $10^2 R_\odot$, the Titius-Bode variable remains sensibly constant. In the typical case $\beta = 0.12$, $\theta_{ph} = 10^{-3}$, for example, $[1 + m(1)/Mf(1)]^2$ increases slowly from about 1.5 at $R_e = 10^4 R_\odot$ to 1.9 at $10^2 R_\odot$. In the same interval the moment-of-inertia coefficient $f(1)$ increases from about 0.007 to 0.017, rising to a maximum value $f_* = 0.022$ at $R_e \simeq 20 R_\odot$.

The observed distribution of orbital radii ratios R_n/R_{n+1} fluctuates randomly from about 1.38 in the case of Earth/Venus to 2.01 for Uranus/Saturn. We have plotted these observed ratios on Figure 13 at each position R_{n+1}. Since $\langle R_n/R_{n+1} \rangle = 1.73 \pm 0.22$ we see that the observed distribution of planetary distances can be safely accommodated in

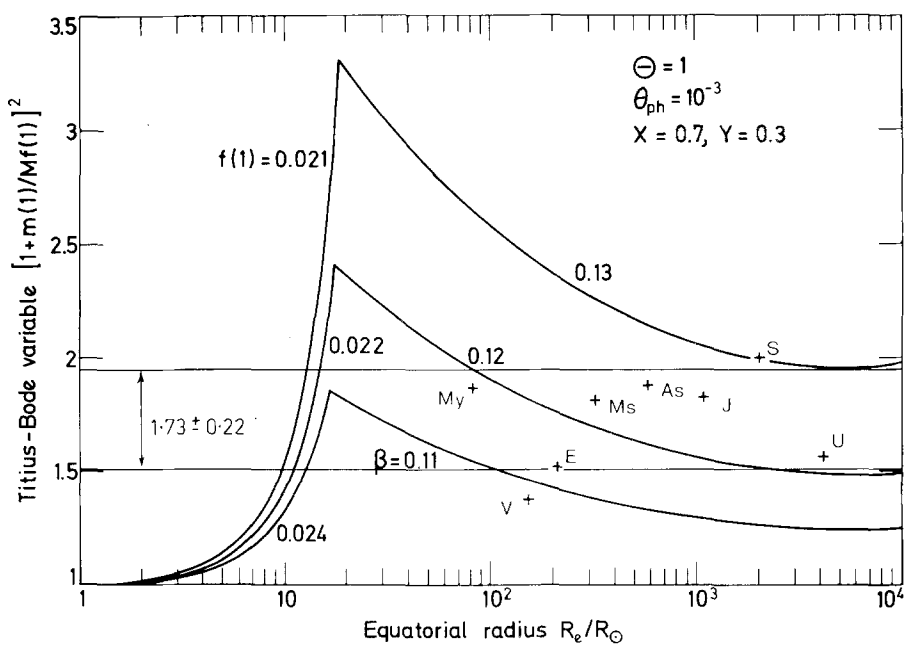

Fig. 13. The Titius-Bode variable $\{1 + m(1)/Mf(1)\}^2$ plotted against equatorial radius R_e for different cases of turbulence parameter β and assuming constant photosurface temperature ratio $\theta_{ph} = 10^{-3}$ (Equation (33)). For $R_e \leqslant R_{e,*} \simeq 20 R_\odot$, where the whole envelope becomes dissociated and $q_1 \to 1$, it is necessary to relax the assumption θ_{ph} = constant since the surface temperature would otherwise become unrealistically high (see Figure 14). Instead we adopt the temperature distribution given by Equation (125) which matches onto the calculations of Ezer and Cameron (1965) and also suppose that the envelope contracts conserving its moment-of-inertia coefficient $f(1) = f(R_{e,*}) \simeq 0.02$ as $R_e \to 1.5 R_\odot$ so that the turbulence dies down.

terms of a model with a turbulence parameter β fluctuating by 10% in the interval 0.11–0.13 with $\theta_{ph} = 10^{-3}$ or, setting $\beta = 0.12$, with θ_{ph} fluctuating within a factor of two of the mean 10^{-3}. {The curve for $\beta = 0.12$, $\theta_{ph} = 0.002$, for example, coincides with the curve $\beta = 0.13$, $\theta_{ph} = 0.001$.} In either case we may safely conclude that the proto-Sun probably did contract more or less homologously in the interval $10^4 R_\odot$ to $10^2 R_\odot$, having typical mean characteristics

$$\langle f(1) \rangle \simeq 0.01, \quad \langle m(1)/M \rangle \simeq 0.003. \tag{128}$$

7.5. SURFACE TEMPERATURE

The variation of surface temperature T_e with R_e also points to the nearly homologous character of the contraction in the interval $10^4 R_\odot$ to $10^2 R_\odot$. During uniform contraction we have $T_e \propto 1/R_e$ which corresponds to a straight line of slope -1 in the log T_e – log R_e diagram. In fact the actual slope of the lines in Figure 14 are slightly less steep than -1, meaning that at larger radii the cloud is slightly warmer than expected on a homologous basis. Physically this relative temperature excess at larger equatorial radii is due to the increased proportion of molecular H_2 in the cloud which raises the mean molecular weight everywhere and hence $T(\propto \mu)$. This variation in T_e due to changing μ becomes particularly noticeable again as R_e approaches $\simeq 20 R_\odot$ where, as the dissociated core moves outwards to the surface of the cloud, the molecular weight in the outermost layers is drastically lowered, thus choking the growth of T_e.

The point $R_{e,*} \simeq 20 R_\odot$ where $q \to 1$ is indicated by a small bar on each line. Below

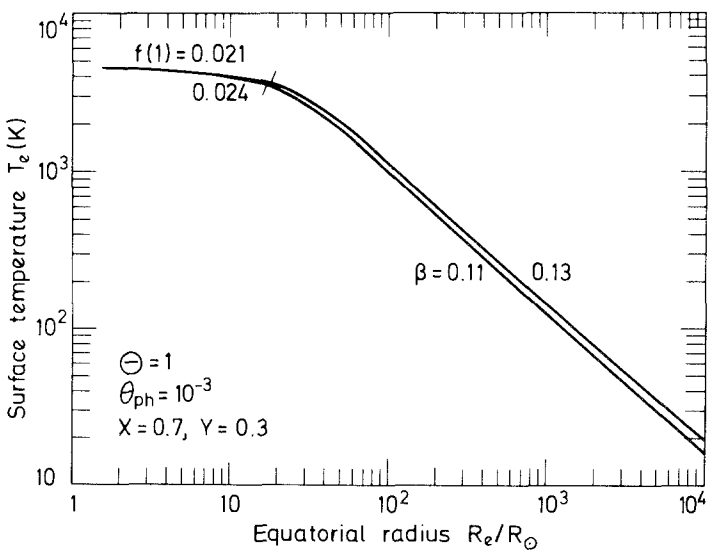

Fig. 14. Surface temperature of the proto-Sun as a function of equatorial radius R_e for different cases of turbulence parameter β, again as described in Figure 13.

this point the photosurface temperature follows the specification given by Equation (125). This final phase of the contraction is extremely non-homologous, at least as far as the outer layers of the proto-Sun are concerned, with θ_{ph} dropping from 10^{-3} to about 10^{-4}. In addition, since the central regions of the turbulent envelope are assumed to contract more or less uniformly so that $f(1)$ remains constant and equal to the value f_* at $R_{e,*}$, we find that the turbulence parameter β falls by a factor of two or so. The mass $m(1)$ of non-turbulent material which can be supported beyond the equatorial cylinder thus declines drastically during the final stage of contraction, causing the gaseous rings disposed at that stage to become progressively more closely spaced together as we note in Figure 13. This is because the contracting envelope is forced to dispose of its excess angular momentum in proportionately smaller and smaller amounts. Since the effective minor radius of each ring, from Equations (124), is $\xi_n \simeq 2R_e/\sqrt{\alpha(1)} \simeq 0.06R_e$, it follows from Figure 13 that once the proto-Sun has contracted to about $3R_\odot$ the subsequently disposed rings become so closely merged that they essentially form a continuous gaseous disc.

7.6. THE RATE OF COLLAPSE

The time $t(R_e)$ taken to complete each stage of the contraction, commencing at radius $10^4 R_\odot$, and given by

$$t(R_e) = \int_{R_e}^{10^4 R_\odot} \mathrm{d}R_e/v_e, \tag{129}$$

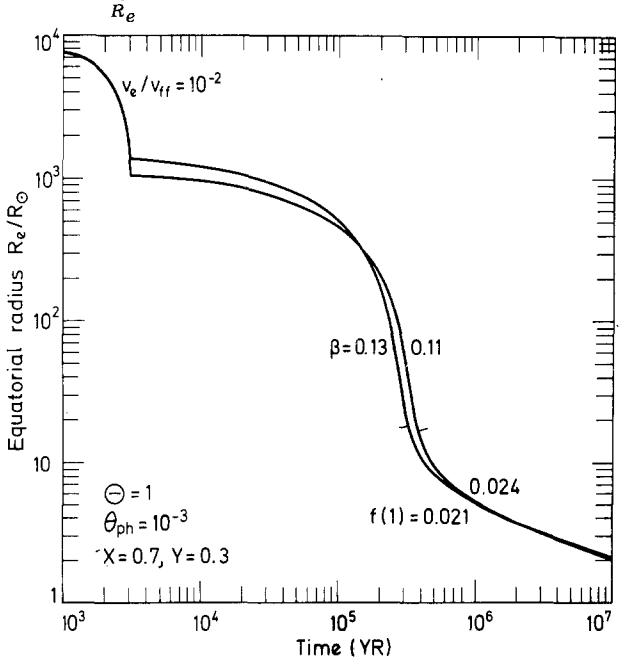

Fig. 15. Equatorial radius of the proto-Sun as a function of time elapsed during the contraction from radius $10^4 R_\odot$, showing the fairly rapid quasi-static phase from radius $10^4 R_\odot$ to $\sim 10^3 R_\odot$ followed by the slow Kelvin-Helmholtz contraction to the zero-age Main Sequence.

where v_e is given by Equations (40) and (42), is plotted in Fig. 15. The first stage of the collapse from $10^4 R_\odot$ to $\sim 10^3 R_\odot$ corresponds to the period of quasi-static equilibrium where the envelope is energetically stabilized through the formation and growth of the small compact embryonic stellar core at the centre of the diffuse cloud. The initial mass of this core is about $0.04 M_\odot$ rising to about $0.08 M_\odot$ as the maximum of the total energy function $E(R_e)$, given by Equation (22) is approached. We set $v_e/v_{ff} = 0.01$ in this interval in accord with Equation (42), where $v_{ff} = (GM/R_e)^{1/2}$ the local 'free-fall' speed. This stage of the collapse is, therefore, fairly rapid; taking only about 3×10^3 yr to be completed.

Below about $10^3 R_\odot$ the contraction of the envelope proceeds much more slowly on a Kelvin-Helmholtz time scale $\tau_{KH} \sim C_n G M^2 / R_e^3 T_e^4$ which for a homologous contraction behaves like $\tau_{KH} \sim R_e$, since $T_e \sim 1/R_e$. Thus the contraction at first proceeds slowly but then quickens as the rate of growth of luminosity due to rising surface temperature overtakes the decrease, due to shrinking surface area. The collapse through the dimensions of the planetary system to about $R_e \simeq 20 R_\odot$ takes about 3×10^5yr to complete.

As soon as the cloud contracts past the turning point $R_{e,*} \sim 20 R_\odot$, indicated by the bars on each line in Figures 14 and 15, the collapse rate begins to slow down markedly. The levelling-off of the surface temperature to 4500 K during this final stage of the contraction causes the surface luminosity $\mathscr{L}_e \propto R_e^2 T_e^4$ rapidly to decline from a maximum of 35 $\mathscr{L}_\odot$ at $R_{e,*}$ to 1 $\mathscr{L}_\odot$ at $R_e \simeq 2 R_\odot$. This decrease in $\mathscr{L}_e$ is accompanied by an increase in the excess gravitational potential energy to be got rid of so that τ_{KH} lengthens drastically. In all, we see from Figure 15 that it takes about 2×10^7yr for the polar radius R_p of the fully rotating proto-Sun to contract to its present size $R_\odot$.

8. Conclusions

We have shown how a typical interstellar cloud fragment of solar mass can safely contract to the size of the planetary system if it is supposed that the various gases of the cloud first condense out as solid grains. Now although it is reasonable to suppose that the CNO component will readily condense out at the temperatures of order 10 K currently expected in cool dark regions of large dense interstellar clouds, we are not sure yet (Reddish, 1975) whether T will fall sufficiently to allow the condensation of H_2 grains.

This stage of the formation process must, therefore, be regarded as being uncertain, though the settling of CNO grains towards the centre of the gas cloud should still occur, nonetheless, thus leading to the desired chemical inhomogeneity considered by Prentice (1976).

Secondly, we have shown how it is possible energetically to stabilize the collapsing solar nebula at a radius $\sim 10^4 R_\odot$ if a small fraction of the central mass falls freely all the way to stellar size forming a small quasi-stellar core of mass ~ 3–$4\% M_\odot$. This core consists primarily of the CNO grains which segregated to the centre of the cloud in the

grain migration era, and so the central chemical inhomogeneity is preserved from being mixed with the turbulent envelope.

Next we have shown how the existence of supersonic convective motions inside the vast energetically stabilized proto-solar envelope allow us to explain why the planetary system is so light in mass compared to the Sun and why the contracting nebula of mass $M \simeq M_\odot$ and moment-of-inertia coefficient $f(1) \simeq 0.01$ disposed of its excess angular momentum through the shedding of a discrete system of gaseous Laplacian rings of nearly constant mass $m(1) \simeq 1000 M_\oplus$, and whose orbital radii R_n satisty a Titius-Bode law relation $R_n/R_{n+1} = [1 + m(1)/Mf(1)]^2 \simeq$ constant. The same result also holds for the gravitational contraction of the primitive gaseous envelopes of Jupiter, Saturn and Uranus, and the formation of the regular satellite systems of these planets (Prentice, 1977).

We have presented simplified polytropic calculations which suggested that the contraction of the protosolar envelope through the dimensions of the planetary system occurred almost homologously, despite the changing mass fraction of H_2 in the cloud. We ignored the presence of the small central compact embryonic core in computing the hydrostatic structure of the envelope but feel that further calculations to include this aspect are in order, especially the construction of a protosolar model to include possible hydrodynamical effects during the period of core growth.

Finally, according to our theory the proto-Sun should have contracted to its present size still spinning quite rapidly with a period of only a few hours. Clearly, therefore, it is necessary to invoke some additional angular momentum braking process such as the interaction of an electrically active solar wind with a strong magnetic field since the Sun's formation to account for the present slow rotation. This consideration does not threaten the validity of the Laplacian hypothesis, however, since the dynamical phase of ring formation which we have described is a very brief and electrically neutral event in the Sun's history taking only some 3×10^5 yr to complete, which is very short compared to the final slow contraction ($\sim 2 \times 10^7$ yr) onto the Main Sequence which, in turn, is extremely short compared to the age of the Sun, some 5×10^9 yr. There is thus enough time left after the planetary formation process has been completed for the Sun to get rid of its final excess of angular momentum.

Acknowledgements

The author is grateful to D. ter Haar for awakening his interest in the origin of the solar system and for offering many helpful comments and discussions during the course of preparation of this manuscript. Part of the work reported here was done with the support of a S.R.C. research associateship position.

References

Alfvén, H. and Arrhenius, G.: 1973, 'Structure and Evolutionary History of the Solar System, III', *Astrophys. Space Sci.* **21**, 117–176.

Allen, C. W.: 1962, *Astrophysical Quantities,* Athlone Press, London.
Babinet, M.: 1861, 'Note sur un point de la cosmogonie de Laplace', *Comptes Rendus Acad. Sci. Paris* **52**, 481–484.
Bodenheimer, P. and Sweigart, A. V.: 1968, 'Dynamical Collapse of the Isothermal Sphere', *Astrophys. J.* **152**, 515–522.
Cameron, A. C. W.: 1962, 'The Formation of the Sun and the Planets', *Icarus* **1**, 13–69.
Cox, J. P. and Guili, R. T.: 1968, *Principles of Stellar Structure,* Vols 1 and 2, Gordon and Breach, New York.
Disney, M. J., McNally, D., and Wright, A. E.: 1969, 'Collapse of Interstellar Gas Clouds – IV. Models of Collapse and a Theory of Star Formation'. *Monthly Notices Roy. Astron Soc.* **146**, 123–160.
Duley, W. W.: 1974, 'Comparison of Grain Mantles in Interstellar Clouds', *Astrophys. Space Sci.* **26**, 199–205.
Engvold, O. and Hauge, Ø.: 1974, 'Elemental Abundances, Isotope Ratios and Molecular Compounds in the Solar Atmosphere', Report No. 39, Institute of Theoretical Astrophys, Blindern-Oslo.
Ezer, D. and Cameron, A. G. W.: 1965, 'A Study of Solar Evolution', *Can. J. Phys.* **43**, 1497–1517.
Freeman, J. W.: 1978, 'The Primordial Solar Magnetic Field', in *The Origin of the Solar System* S. F. Dermott, ed.), John Wiley & Sons, London (in press).
Grossman, L. and Larimer, J. W.: 1974, 'Early Chemical History of the Solar System', *Revs. Geophys. Space Phys.* **12**, 71–101.
Hayashi, C.: 1961, 'Stellar Evolution in Early Phases of Gravitational Contraction', *Publ. Astron. Soc. Japan* **13**, 450–452.
Hollenbach, D. and Salpeter, E. E.: 1971, 'Surface Recombination of Hydrogen Molecules', *Astrophys. J.* **163**, 155–164.
Hoyle, F.: 1955, *Frontiers of Astronomy,* Heineman, London.
Hoyle, F.: 1960, 'On the Origin of the Solar Nebula', *Quart. J. Roy. Astron. Soc.* **1**, 28–55.
Hoyle, F. and Wickramasinghe, N. C.: 1968, 'Condensation of the Planets', *Nature* **217**, 415–418.
James, R.: 1964, 'The Structure and Stability of Rotating Gas Masses', *Astrophys. J.* **140**, 552–582.
Jeans, J. H.: 1928, *Astronomy and Cosmogony,* Cambridge University Press, Cambridge.
Kuiper, G. P.: 1951, 'On the Origin of the Solar System', in *Astrophysics* (J. A. Hynek, ed.), pp.357–424. McGraw-Hill, New York.
Laplace, P. S. de: 1796, *Exposition du Système de Monde,* Courcier, Paris.
Larson, R. B.: 1969, 'Numerical Calculations of the Dynamics of a Collapsing Proto-Star', *Monthly Notices Roy. Astron. Soc.* **145**, 271–295.
Lewis, J. S.: 1974, 'The Temperature Gradient in the Solar Nebula', *Science* **186**, 440–443.
Maxwell, J. C.: 1855, 'On the Stability of the Motions of Saturn's Rings', in *Scientific Papers of J. C. Maxwell* (W. D. Niven, ed.), pp. 288–376, Dover, New York.
Mestel, L.: 1965a, 'Problems of Star Formation – I', *Quart. J. Roy. Astron. Soc.* **6**, 161–198.
Mestel, L.: 1965b, 'Problems of Star Formation – II', *Quart. J. Roy. Astron. Soc.* **6**, 265–298.
Monaghan, J. J. and Roxburgh, I. W.: 1965, 'The Structure of Rapidly Rotating Polytropes', *Monthly Notices Roy. Astron. Soc.* **131**, 13–21.
Nieto, M. M.: 1972, *The Titius-Bode Law of Planetary Distances: Its History and Theory,* Pergamon Press, Oxford.
Penston, M. V.: 1966, 'Dynamics of Self-Gravitating Gaseous Spheres. I. The Collapse of an Isothermal Gaseous Sphere', *Roy. Obs. Bull.,* No. 117.
Poincaré, H.: 1911, *Leçons sur les Hypothèses Cosmogoniques,* Herman, Paris.
Prentice, A. J. R. and ter Haar, D.: 1971, 'On the Angular Momentum Problem in Star Formation', *Monthly Notices Roy. Astron. Soc.* **151**, 177–184.
Prentice, A. J. R.: 1973, 'On Turbulent Stress and the Structure of Young Convective Stars', *Astron. Astrophys.* **27**, 237–248.
Prentice, A. J. R.: 1976, 'Supersonic Turbulent Convection, Inhomogeneities of Chemical Composition, and the Solar Neutrino Problem', *Astron. Astrophys.* **50**, 59–70.
Prentice, A. J. R.: 1977, 'Formation of the Satellite Systems of the Major Planets', *Proc. Astron. Soc. Australia* **3**, 172–173.

Reddish, V. C.: 1975, 'Star Formation in Clouds of Molecular Hydrogen', *Monthly Notices Roy. Astron. Soc.* **170,** 261–280.

Reddish, V. C. and Wickramasinghe, N. C.: 1969, 'Star Formation in Clouds of Solid Hydrogen Grains', *Monthly Notices Roy. Astron. Soc.* **143**, 189–208.

Roxburgh, I. W.: 1966, 'On the Fission Theory of the Origin of Binary Stars', *Astrophys. J.* **143,** 111–120.

Schatzman, E.: 1949, 'On Certain Paths of Stellar Evolution. I – Preliminary Remarks', *Bull. Acad. Roy. Belgique* **35,** 1141–1152.

Schatzman, E.: 1967, 'Cosmogony of the Solar System and the Origin of Deuterium', *Ann. Astrophys.* **30,** 963–973.

Schatzman, E.: 1971, in *Highlights of Astronomy* (C. de Jager, ed.), Vol. 2, p. 197, D. Reidel, Dordrecht, Holland.

Schmidt, M.: 1965, 'Rotation Parameters and Distribution of Mass in the Galaxy', in *Stars and Stellar Systems* (A. Blaauw and M. Schmidt, eds.), pp. 513–530, University of Chicago Press, Chicago.

Spitzer, L.: 1968, *Diffuse Matter in Space,* Interscience, New York.

ter Haar, D.: 1948, 'Studies on the Origin of the Solar System', *Proc. Roy. Danish Acad. Sci.* **25,** No. 3.

ter Haar, D.: 1950, 'Further Studies on the Origin of the Solar System', *Astrophys. J.* **111,** 179–190.

ter Haar, D.: 1967, 'On the Origin of the Solar System', *Ann. Rev. Astron. Astrophys.* **5,** 267–278.

ter Haar, D. and Cameron, A. G. W.: 1963, 'Historical Review of Theories of the Origin of the Solar System', in *Origin of the Solar System* (R. Jastrow and A. G. W. Cameron, eds.), pp. 4–37, Academic Press, New York.

Urey, H. C.: 1951, 'The Origin and Development of the Earth and Other Terrestrial Planets', *Geochim. Cosmochim. Acta* **1,** 209–277.

Weber, E. J. and Davis, L. Jr.: 1967, 'The Angular Momentum of the Solar Wind', *Astrophys. J.* **148,** 217–227.

Whipple, F. L.: 1972, *Earth, Moon and Planets,* Harvard University Press, Cambridge Mass.